DECODING FOUR-FINGER PROPRIOCEPTIVE AND TACTILE STIMULI FROM MAGNETOENCEPHALOGRAPHY

Paavo Nyländen

Master`s Thesis in Biomechanics
Faculty of Sport and Health Sciences
University of Jyväskylä
Spring 2024

TIIVISTELMÄ

Nyländen, P. 2023. Sormien tunto- ja proprioseptiivisten ärsykkeiden erottelu aivomagneettikäyrästä. Liikuntatieteellinen tiedekunta, Jyväskylän yliopisto, (biomekaniikka) pro gradu -tutkielma, 47 s., 1 liite.

Tämän tutkimuksen tavoitteena oli tutkia sormiin kohdistuvien tunto- ja proprioseptiivisten ärsykkeiden erottelua aivomagneettikäyrästä (MEG) käyttämällä tukivektorikonetta (SVM). Neuroproteeseissa käytettyjen aivo-tietokonerajapintojen (BCI) toiminnan kehittymisen kannalta on tärkeää pystyä erottelemaan hienovaraisia sensorisia ärsykkeitä aivosignaaleista. Tässä tutkimuksessa tarkasteltiin näiden ärsykkeiden temporaalisten MEG-vasteiden käyttöä binäärisessä luokittelussa.

Tutkimukseen osallistui kymmenen tervettä aikuista. Tutkittavat istuivat MEG-laitteessa toinen käsi tunto- ja liikeärsykkeitä sormiin antavan pneumaattisen laitteen päällä. MEG-data tallennettiin käyttäen 306-kanavaista Elekta Neuromag -järjestelmää 1000 Hz:n näytteenottotaajuudella. MEG-signaalien esikäsittelyssä käytettiin useita vaimennustekniikoita, kuten ajallista projektiota (OTP), ajallista erottelua (tSSS) ja itsenäisten komponenttien analyysia (ICA). Erottelua varten piirteet poimittiin MEG-signaalien ajallisista muutoksista liukuvaa aikaikkunaa käyttäen. Luokittelussa käytettiin standardia tukivektorikonetta ja ristiin validointia (*5-fold cross-validation*).

Tulokset osoittivat, että eri sormiin annetut proprioseptiiviset ärsykkeet tuottivat korkeampia ja johdonmukaisempia luokittelutarkkuuksia (70–73%) verrattuna tuntoärsykkeisiin (noin 67–72%). Proprioseptiivisten ja tuntoärsykkeiden erottelu toisistaan, kun ne kohdistettiin samaan sormeen, saavutti keskimäärin noin 90 % luokittelutarkkuuden. Näiden havaintojen perusteella voidaan todeta, että MEG-signaalien ajallisia vasteita voidaan tehokkaasti käyttää aistiärsykkeiden erottelussa. Jatkossa vastaavien tutkimusten tulisi harkita suuremman otoksen ja erilaisten piirteenvalintamenetelmien käyttämistä sekä elektroenkefalografian (EEG) hyödyntämistä käytännöllisyyden vuoksi.

Asiasanat: aivomagneettikäyrä, proprioseptiikka, tuntoärsyke, tukivektorikone

ABSTRACT

Nyländen, P. 2023. Decoding four-finger proprioceptive and tactile stimuli from magnetoencephalography, University of Jyväskylä, Master's thesis, 47 pp., 1 appendix.

This study aimed to investigate the feasibility of decoding proprioceptive and tactile stimuli applied to the fingers using magnetoencephalography (MEG) signals and support vector machines (SVMs). With the advancement of neuroprosthetic brain-computer interfaces (BCIs) there is a growing need to enhance the control of these devices by accurately decoding subtle sensory stimuli. This research focuses on the temporal dynamics of MEG responses to such stimuli, investigating their potential to inform the development of more dexterous and responsive neuroprostheses.

The method involved recruiting ten healthy adult participants and using a custom-built four-finger pneumatic actuator integrated with a tactile stimulator to deliver stimuli to the index, middle, ring, and little fingers. MEG data were recorded using a 306-channel Elekta Neuromag system at a 1000 Hz sampling rate. Preprocessing steps included noise reduction techniques such as oversampled temporal projection (OTP), temporal signal space separation (tSSS), and independent component analysis (ICA). Features for decoding were extracted from the temporal changes in MEG signals using a sliding time window analysis, and SVMs were employed for classification.

Results indicated that proprioceptive stimuli applied to different fingers yielded slightly higher and more consistent classification accuracies (70%-73%) compared to tactile stimuli (around 67%-72%). Classification between proprioceptive and tactile stimuli applied to the same finger achieved even higher accuracies, averaging around 90%. These findings suggest that the temporal characteristics of MEG signals can be effectively used for decoding sensory stimuli, providing a solid foundation for future BCI applications. Further research should consider expanding the sample size, exploring different feature selection methods, and utilizing electroencephalography (EEG) for practical, non-invasive BCI implementations.

Key words: magnetoencephalography, proprioception, tactile stimuli, support vector machine

ABBREVIATIONS

BCI	brain-computer interface
EEG	electroencephalography
ERD/ERS	event-related de-/synchronisation
ICA	independent component analysis
MEG	magnetoencephalography
MLP	multilayer perceptron
MRCP	movement-related cortical potential
MSC	magnitude squared coherence
OTP	oversampled temporal projection
PLV	phase locking value
SQUID	superconducting quantum interference device
tSSS	temporal signal space separation
LDA	linear discriminant analysis
SVM	support vector machine

CONTENTS

1 INTRODUCTION

The advancement of real-time neuroprosthetic brain-computer interfaces (BCIs) has made it possible for paralyzed patients and amputees to restore limb function. This is accomplished by utilizing machine learning algorithms to decode users' intentions from brain signals and by using that information to direct prosthetic limbs or electrical stimulations to muscles. For instance, magnetoencephalography (MEG) or electroencephalography (EEG) can be used to measure brain signals during imagined movements, and features extracted from these signals, like frequency characteristics, can be used as input for the algorithms in order to predict the intended movements. (Nason et al. 2021) A schematic showing the function of a neuroprosthetic BCI is presented in Figure 1.

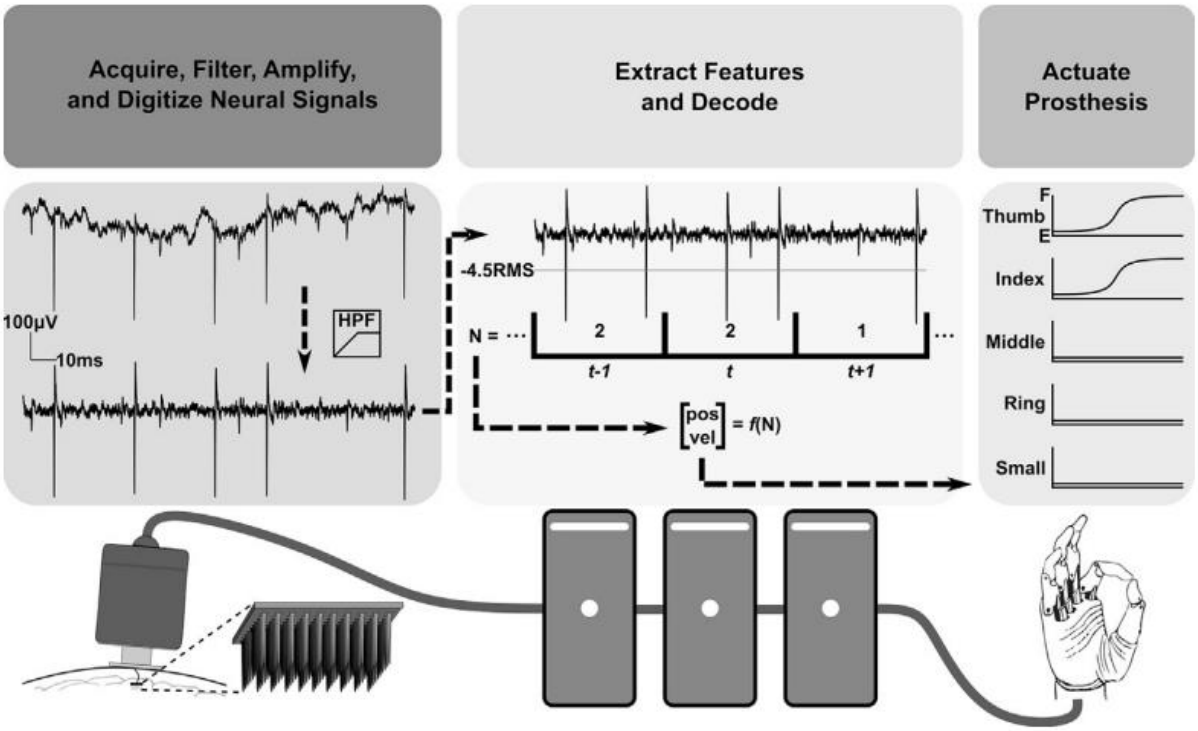

FIGURE 1. Information processing in a neuroprosthetic BCI (Nason et al 2021).

At present, these neuroprosthetic devices have demonstrated success mainly in laboratory environments (Nason et al. 2021). One of the most significant proof-of-concept studies was conducted by Ajiboye and colleagues (2017) who showed that restoration of whole-arm reaching and grasping movements was possible for a tetraplegic patient. The patient had a high-cervical spinal cord injury that had resulted in complete loss of arm and hand function.

With microelectrode arrays placed on the motor cortex for signal acquisition and percutaneous stimulation electrodes placed on the upper and lower arm for muscle activation, the patient was eventually able to perform simple grasping actions voluntarily.

Implanted electrodes can record signals from small neuronal populations and thus provide a spatially accurate method for signal acquisition. Because MEG and EEG signals are recorded from the scalp, their spatial resolution is significantly worse compared to implantable electrodes. (Waldert et al. 2009) However, implanting an electrode under the skull has a risk of causing complications like surgical site infections (Kantzanou et al. 2021). Therefore, as non-invasive methods, MEG and EEG provide a safer alternative for neuroprosthetic BCIs.

For more precise control of a neuroprosthesis, the ability to decode subtle movements, like finger flexion and extension, is needed. In addition, as suggested by Ajiboye et al. (2017), restored somatosensation could enhance the diversity of these devices by allowing users to perform movements without visual feedback. Therefore, accurate decoding of proprioceptive and tactile stimuli applied to the fingers holds the potential to foster the development of dexterous neuroprostheses. The objective of this study is to investigate the feasibility of decoding finger movements and light touches induced by a pneumatic device using MEG for signal acquisition.

In order to gain a comprehensive understanding of the topic, the next chapters cover the basics of MEG as a brain imaging method as well as the machine learning algorithms that are used for information decoding. In addition, one chapter is devoted to the neural processes that constitute the perception of proprioceptive and tactile stimuli. Finally, these elements are brought together to look at the latest research in the field of sensorimotor decoding.

2 ELEMENTS OF MAGNETOENCEPHALOGRAPHY

MEG is a non-invasive brain imaging method that enables real-time measurements of brain activity by recording weak magnetic fields generated by neurons (Hämäläinen 1992; Hämäläinen et al. 1993). Compared to electrical currents measured by EEG, these magnetic fields have a unique advantage in that they are not attenuated or distorted by tissues between the signal sources and the recording sensors (Baillet 2017). The main component of an MEG sensor is a superconducting quantum interference device (SQUID) which transforms magnetic fields into currents by electromagnetic induction (Hämäläinen et al. 1993). They were first introduced by Zimmerman et al. (1970) while preliminary measurements of the brain's magnetic fields with these devices were done by Cohen et al. (1972).

Currently, MEG is strongly present in neuroscientific research and its significance in bringing together different brain imaging methods is increasing as there are various other methods that can be used simultaneously with it (Baillet 2017). In the following sections, a more comprehensive look at MEG signal genesis, instrumentation and data analysis is provided.

2.1 Signal genesis

Electrical currents in the form of action potentials are produced in the neurons of the brain by rapid fluxes of sodium and potassium ions through voltage-gated ion channels located on the cell membrane (Hodgkin 1951). In addition, neurons exhibit postsynaptic dendritic currents. Both currents give rise to a magnetic field (Hämäläinen et al. 1993).

A primary current in the dendrite of a neuron can be approximated with a current dipole (Figure 2) (Hämäläinen et al. 1993). Due to their elongated morphology, thousands of parallel axons firing simultaneously can create a high enough magnetic field to be detected in the MEG, while cells with a more stellate structure can't (Baillet 2017). The densities of biological magnetic fields vary from 50 to 500 fT. MEG sensors are mostly sensitive to magnetic fields produced by primary currents tangential to the scalp surface. (Hämäläinen et al. 1993)

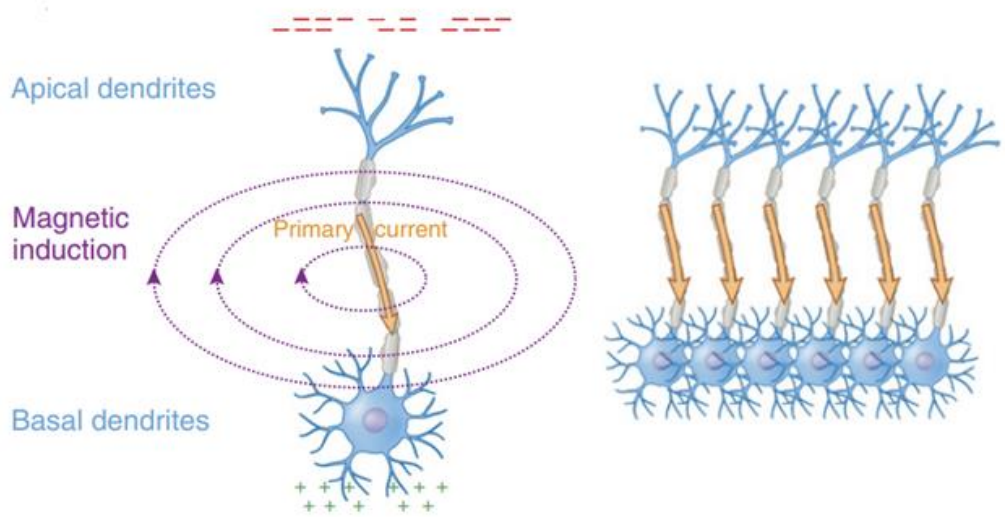

FIGURE 2. Current dipoles of primary currents and resultant magnetic fields in cortical neurons (adopted from Baillet 2017).

2.2 Instrumentation

To record the neuronal magnetic fields, a proper magnetically shielded facility is needed in addition to the MEG device itself. The MEG site's noise conditions determine the necessary requirements; rural or magnetically quiet sites require less shielding compared to urban sites where low-frequency drift and power line noise are more common. (Lee & Kim 2014) A diagram showing all the components of an MEG system is shown in Figure 3.

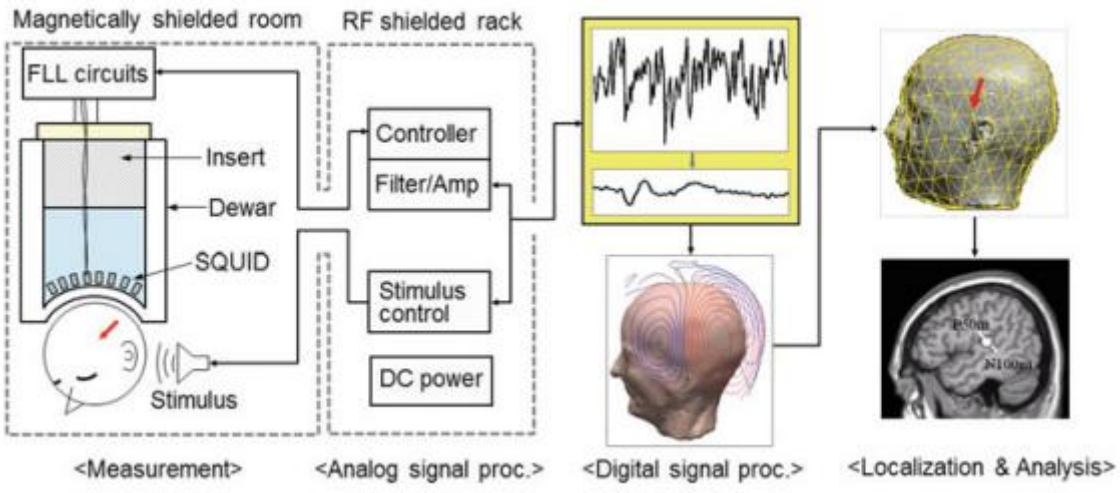

FIGURE 3. Components of an MEG system (Lee & Kim 2014).

While SQUIDs are extremely sensitive, they are not able to directly pick up magnetic fields from the human brain because they must be relatively small. This is where pickup coils come into play. A pickup coil, also known as a flux transformer, is a component that can amplify the magnetic fields and transmit them to the SQUID sensor. The pickup coil is designed with a much larger diameter than the SQUID loop, which allows it to effectively capture magnetic fields from the brain. The pickup coil is integrated with an input coil that is directly attached to the SQUID loop. This setup creates a superconductive flux transformer circuit that can effectively convert the screening current generated in the pickup coil into magnetic flux through the input coil. This amplified magnetic flux signal is then detected by the SQUID sensor (Figure 4). (Cohen et al. 1972; Hämäläinen et al. 1993; Ryhönen et al. 1989)

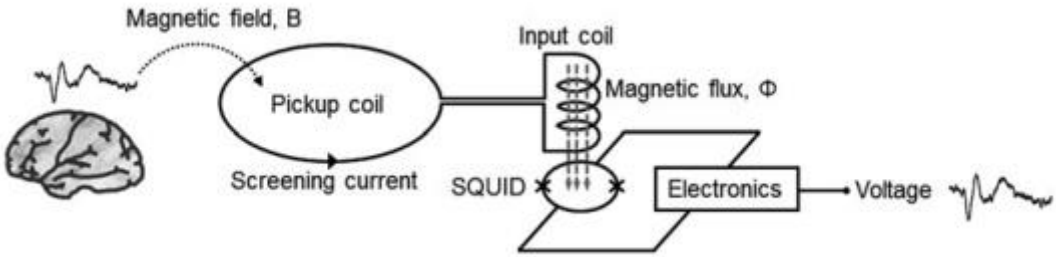

FIGURE 4. Operating principle of an MEG sensor (Lee & Kim 2014).

There are a couple of different pickup coil configurations that can be used in addition to the single loop coil, or magnetometer, presented in Figure 4 (Hämäläinen et al. 1993). Planar and axial first order gradiometers, where two of these magnetometers are connected together, can be used to reduce noise or increase sensitivity to deep sources of the brain. Regardless of the configuration used, the entire circuit needs to be cooled to an extremely low temperature to decrease electromagnetic resistance. This is usually achieved with liquid helium inside the dewar. In addition, flux-locked loop (FLL) circuits are needed to linearize the SQUID sensors' periodic output (Lee & Kim 2014).

2.3 Analyzing MEG data

MEG data represents the rapidly changing magnetic fields of the brain. Even during rest, there is ongoing activity in different brain regions that can be seen as oscillatory signals in real-time. External stimuli, like auditory cues, can cause event-related responses that appear as time-locked amplitude changes in these signals. Due to this nature, MEG data can be viewed in both the time-domain, where the signal power is plotted against time, and the frequency-domain, where the signal power is plotted against the frequency components that make up the oscillations. These two dimensions can also be viewed together in the time-frequency-domain. (Gross et al. 2013; Hämäläinen et al. 1993)

A crucial step before data analysis is artifact removal and noise reduction. Artifact rejection techniques include for example, manual rejection, independent component analysis (ICA) and signal space separation. ICA is commonly used to detect signal components that are caused by blinks and eye movements. However, some of these techniques have drawbacks like signal loss and are therefore better suited for certain experimental setups than others. (Haumann et al. 2016)

2.3.1 Time-domain features

An example of a traditional time-locked event-related response is the P300 (or P3) response which refers to a positive amplitude spike approximately 300 ms after a stimulus onset (Sutton et al. 1965). It was first discovered with EEG but later its magnetic equivalent was introduced as well (Alho et al. 1998). Another event-related response that can be seen with MEG is mismatch negativity caused by deviant auditory stimuli that are presented randomly among standard repetitive sounds. A similar response to a change of stimulus can be seen in somatosensory modalities. (Näätänen et al. 2007)

Brenner et al. (1978), Hari et al. (1984) and Okada et al. (1984) carried out early studies that used event-related responses to somatosensory stimuli in MEG to investigate the organization of the sensory cortices. These studies found evidence for different representations of body parts, especially fingers, in the primary somatosensory cortex.

2.3.2 Frequency- and time-frequency-domain features

The oscillatory activity of the brain can be separated into its constituent frequency bands. These include delta (2 – 4 Hz), theta (4 – 8 Hz), alpha (8 – 12 Hz), beta (15 – 30 Hz), lower gamma (30 – 80 Hz) and upper gamma (80 – 150 Hz) bands. (Cohen 2014, 33) These bands are resulted from different signal transmission dynamics in the brain and therefore carry information related to specific neural processes (Buzsaki & Draguhn 2004).

Each frequency band expresses unique behavior in response to an event. Alpha band shows power decrease (desynchronization) relative to a resting state band power during cognitive and memory tasks. Theta band, on the other hand, works in the opposite way. (Klimesch 1999; Hämäläinen et al. 1993) During motor tasks and motor imagery, alpha and theta power decrease with a simultaneous increase in gamma power (Miller et al. 2007; Miller et al. 2010). Figure 5 illustrates the differences between the MEG signal domains.

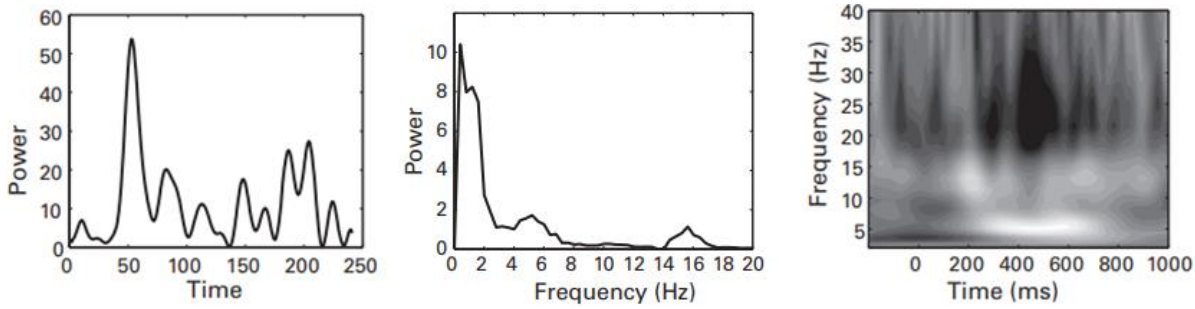

FIGURE 5. Dimensions of MEG data. Brightness portrays signal power in the time-frequency graph (right) (adopted from Cohen 2014, 36).

3 NEURAL PROCESSING OF PROPRIOCEPTIVE AND TACTILE STIMULI

Sensory processing is a complex and essential process that allows us to interact with the world around us. In order to decode sensory information using MEG, it is important to understand the underlying structural and functional aspects of sensory perception. This chapter provides a brief overview of the neurophysiology involved in somatosensory processing, with a particular focus on the differences between pathways that convey proprioceptive and tactile information.

Proprioception refers to the body's ability to sense its position and movement without relying on visual feedback. This crucial function is primarily mediated by muscle spindles, specialized sensory receptors located within the skeletal muscles. (Proske & Gandevia 2012) When muscles stretch, muscle spindles activate Ia afferent nerve fibers (or primary afferent fibers), which are synapsed onto alpha motoneurons in the spinal cord. This results in a rapid contraction of the same muscle fibers, which is known as the stretch reflex. (Matthews 1991) This feedback loop allows immediate muscle length adjustments and contributes to the maintenance of body posture. In addition to the stretch reflex, afferent feedback from muscle spindles is also inherently involved in the ongoing perception of joint position. While the function of Golgi tendon organs in proprioception is less clear, some evidence suggest that they might be involved as well. (Proske & Gandevia 2012)

A tactile stimulus activates specialized cutaneous receptor cells connected to Aβ afferent nerve fibers (Purves et al. 2018, 194-195). Each of these receptor cells responds to a specific type of stimulation, such as edges, blunt objects, or skin movements (Hunt & McIntyre, 1960; Iggo & Muir, 1969; Johansson & Flanagan, 2009). Merkel cells, located at the tip of the intermediate epidermal ridges, are the ones responsible for mediating sensations of light touch and pressure (Johansson & Vallbo 1983). Interestingly, the role of cutaneous receptors in proprioception has also been debated (Chambers et al., 1972; Edin, 1992; Edin, 2004). One notable difference between cutaneous receptors and muscle spindles is that action potentials from cutaneous receptors are conducted to the spinal cord at a slower rate than those from muscle spindles due to the smaller axon diameter of Aβ afferents (Shefner & Logician 1994).

From the spinal cord, somatosensory signals are conveyed to supraspinal structures through ascending pathways. Proprioceptive afferents bifurcate and send collateral branches to several

spinal segments from where they ascend through medial lemniscus and dorsal spinocerebellar tract. Second-order neurons from the brainstem then carry over to the contralateral ventral posterior lateral nucleus of the thalamus and to the cerebellum. Tactile afferents ascend only through medial lemniscus with second-order neurons projecting to the thalamus as well. Finally, third-order neurons originating from the thalamus send their axons to the primary somatosensory cortex. (Purves et al. 2018, 203-205)

In addition to its topographical distribution, the primary somatosensory cortex is organized into four distinct regions known as Brodmann's areas 3a, 3b, 1, and 2 (Figure 6), each of which is responsible for processing different types of sensory information. Areas 3b and 1 are predominantly responsible for processing cutaneous stimuli, area 3a processes proprioceptive stimuli, while area 2 processes both, with the majority of thalamic projections entering area 3b. (Graziano & Gross 1998; Kaas et al. 1993) The secondary somatosensory cortex receives plenty of connections from all of these areas while area 2 provides further connections to posterior parietal areas that eventually lead to motor cortices (Purves et al. 2018, 208).

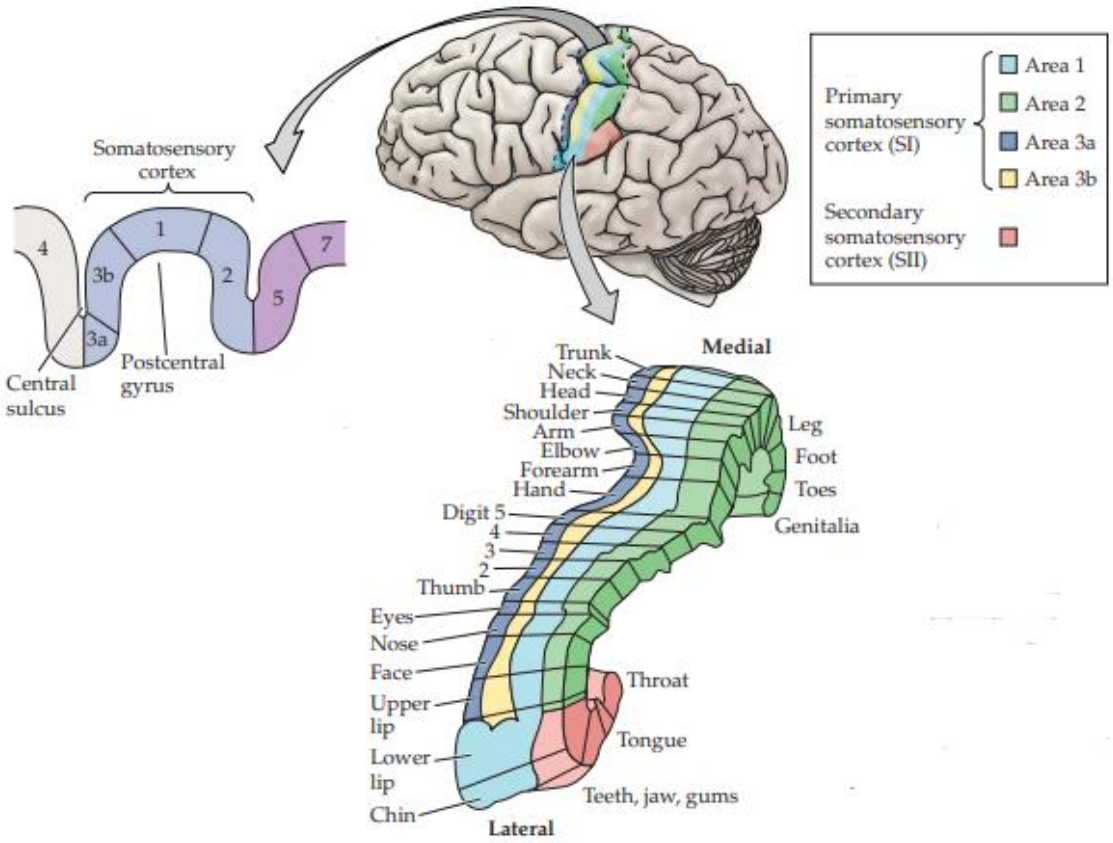

FIGURE 6. The organization of the somatosensory cortices (adopted from Purves et al. 2018, 206).

4 MACHINE LEARNING ALGORITHMS FOR INFORMATION DECODING

A machine learning algorithm can be defined as a computational procedure intended to derive predictions based on data which has been used to train it. Central to these algorithms are two fundamental components: a hypothesis and a loss function. The hypothesis represents the underlying assumptions made by the model regarding the relationships among the variables within the data. The loss function, on the other hand, serves as a metric for estimating the error or discrepancy between the model's predictions and the actual outcomes. Machine learning algorithms fit the hypothesis to the data by minimizing the loss function. (Jung 2022, 19-39) In the context of sensorimotor decoding, this might mean that the model learns to predict movements using, for example, spatial or temporal characteristics of event-related responses as its input data. Due to the vastness of this field, this chapter explains only the most relevant methods that are being used in BCI applications.

4.1 Classical methods

Linear regression. In linear regression, the relationship between a dependent variable (Y) and a set of independent variables (X) is modeled through a linear equation. The dependent variable is expressed as the sum of the product of the independent variables and their corresponding regression coefficients (B). This can be mathematically represented as $Y_i = B_1 + B_2X_{2i} + B_3X_{3i} + \cdots + B_kX_{ki} + u_i$, where B_1 denotes the intercept term (representing the mean value of Y when X_2 to X_k are zero), B_2 to B_k represent the partial regression coefficients, and u_i denotes the error term. The error term quantifies the discrepancy between the actual values and the estimated values (u = Y – BX) which means that by minimizing it the optimal regression coefficients can be found. To mitigate the issue of positive and negative errors offsetting each other in this process, the ordinary least squares method can be used ($\sum {u_i}^2 = \sum(Y_i - B_1 - B_2X_{2i} - B_3X_{3i} - \cdots - B_kX_{ki})^2$. This formulation results in a linear relationship between the dependent variable and the independent variables. (Gujarati 2018)

Support vector machines. A similar hypothesis is also exploited in support vector machines (SVM) which are used to categorize data. The general idea is to establish a hyperplane within a two-dimensional (or a multi-dimensional) space that effectively delineates observations into

two distinct categories. This hyperplane is mathematically represented as the function $y(x) = w^T x + b$, where the sign of the resulting value determines the binary classification label. The error is minimized by maximizing the distance between the support vectors responsible for separating the observations. The more separation between the groups the less error there is in the estimation. A kernel trick can be used to make the hypothesis function non-linear and fit into more challenging data. (Suykens et al. 2002, 29-36)

Linear discriminant analysis. Linear discriminant analysis (LDA) is a technique utilized to separate two or more classes using a linear hyperplane. Its distinction from SVMs lies in the way the hyperplane is positioned, aiming to maximize the inter-group mean distance while minimizing intra-group variation or scatter. In the context of classifying multiple categories, the distances between means are computed from the central point of the space. (Tharwat et al. 2017)

K-nearest neighbors. Unlike the previous three, the k-nearest neighbors algorithm can be used for both regression and classification. Given a new data point, the algorithm identifies the k closest data points (using the training data) to that point in the feature space based on their Euclidean distance. The class or value of the new data point is then determined by majority ruling or averaging the labels or values of its k nearest neighbors. In classification tasks, the label that appears most frequently among the nearest neighbors becomes the predicted class for the new data point, while in regression tasks, the predicted value is computed as the average or weighted average of the values from the nearest neighbors. A small value of k may encompass noise or be influenced by outliers, whereas a large value of k may disregard classes with limited data points. (Jung 2022, 75)

4.2 Artificial neural networks

Artificial neural networks mimic the information processing of the brain because they are built as networks of interconnected nodes or neurons. There are various types of architectures for these networks but one of the simplest one is called a multilayer perceptron (MLP). (Nielsen 2015) An MLP is a feed-forward neural network, meaning information flows in one direction; from the input layer through the hidden layers to the output layer (Figure 7). The input layer receives the data, which can be represented as a vector of input values, each node

therefore receiving one input. Each input value corresponds to a specific feature or attribute of the input data. One or more hidden layers are located between the input layer and the output layer. Hidden layers consist of multiple nodes, and the outputs from nodes in one hidden layer serve as inputs to the nodes in the subsequent hidden layer. (Murtagh 1991)

Each connection in the network is associated with a weight. These weights determine the strength or importance of the connection. Additionally, each node (except those in the input layer) has a bias, which is a constant value that affects the overall output of the node. In each node, the weighted sum of the inputs is calculated by multiplying each input value by its corresponding weight and summing the results. The weighted sum can be expressed as $Z = w_1x_1 + w_2x_2 + \ldots + w_n * x_n + b$. The weighted sum (Z) is then passed through an activation function, which introduces non-linearity into the output of the node. The output layer can consist of one or multiple nodes, depending on the specific task at hand. The outputs from these nodes represent the network's predictions. The training of an MLP involves adjusting the weights and biases through backpropagation to minimize the difference between the network's predicted outputs and the desired outputs. (Murtagh 1991)

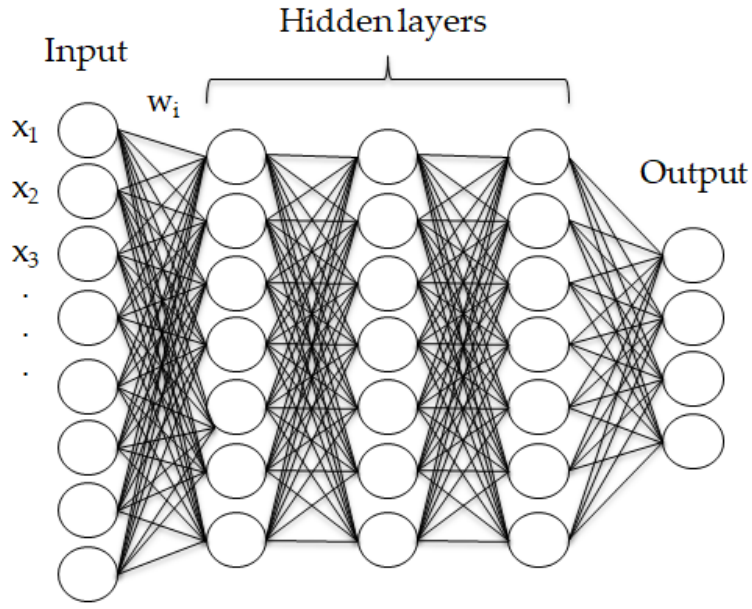

FIGURE 7. Diagram illustrating the architecture of an artificial feed-forward neural network, where the layer sizes can be flexible. Deep learning networks often consist of numerous large hidden layers. (Adopted from Jung 2022, 73)

5 DECODING SENSORIMOTOR INFORMATION FROM BRAIN SIGNALS

This chapter merges together the preceding topics of brain signal acquisition and machine learning to examine how previous studies have investigated the decoding of sensorimotor information. It should be noted that most studies in this field have utilized only EEG, likely due to its inexpensiveness and portability. Consequently, only a limited number of high-quality studies involving MEG are included in this chapter.

Sensorimotor decoding can be approached either as a classification problem or a regression problem, depending on the task and machine learning algorithms used. In classification problems, the objective is to categorize movements or stimuli into predefined groups, such as "index finger extension" or "middle finger flexion." Regression problems involve decoding of continuous variables, such as the velocity of a limb. Features and methods that achieve the highest accuracy can differ between these approaches.

5.1 Movement classification

In a study conducted by Schwarz and colleagues (2018), participants were instructed to perform three distinct grasping actions (palmar, pincer, and lateral grasp). Each task was repeated 72 times in a randomized order with the aid of auditory cues. A pressure button was employed during resting periods to synchronize the onset of movement with EEG recordings. The time region of interest (tROI) spanned from -2 seconds to 3 seconds, with 0 seconds denoting the movement onset recorded by the pressure button. Movement-related cortical potentials (MRCPs) derived from band-pass filtered data (0.3 - 3 Hz) were utilized as features. For both binary and multiclass classification, shrinkage linear discriminant analysis (sLDA) was employed.

On average the decoding accuracy (the ratio of correctly classified instances to the total number of instances) increased significantly towards the movement onset. Accuracy for all movement conditions against the no-movement state surpassed 93% in the time region of 0 to 1 second. Furthermore, in all multiclass conditions the accuracy exceeded 50% when the same tROI was used. (Schwarz et al. 2018)

Two similar studies were conducted by Xu et al. (2021a, 2021b). In their initial study, participants performed a pinch grasp, a palmar grasp, and a precision disk rotation in four different conditions. In the first condition, they gradually increased grasping force over three seconds to reach 60% of the maximal force. The second condition was similar, except the force was increased within 0.5 seconds. The remaining two conditions followed the same procedure but with 20% of the maximal force. MRCPs were extracted from a low-pass filtered EEG using a one-second sliding time window with a step size of 100 milliseconds. For fast movements, a tROI of -1s to 4s was chosen, while for slow movements, it was set to -1s to 6s. Classification was performed using sLDA. (Xu et al. 2021a).

A binary classification between all the grasping actions showed similar accuracy in both fast and slow conditions. Interestingly, the variance in accuracies between the subjects and the intra-subject conditions was relatively high. On average the rotation movement showed weakest results. (Xu et al. 2021a) In their second study, Xu and colleagues (2021b) expanded their research by incorporating additional grasping actions without the use of force levels. With a total of five actions (palmar, pinch, push, twist and plug) the classification accuracy still exceeded the chance level (20%) in all conditions.

In addition to the EEG studies that have used time-domain features, frequency characteristics of MEG have also been used for movement classification. Waldert et al. (2008) had their subjects manipulate a joystick in four planar directions (forwards, backwards, left, and right) while normalized powers of MEG frequency bands were used as inputs for a regularized linear discriminant classifier (rLDA). Sensors placed over the motor areas exhibited significant power modulation in three frequency bands: an increase in < 7 Hz and 62-87 Hz, and a decrease in 10-30 Hz. However, as expected, the low frequency features performed best with average classification accuracies falling just under 40%.

One of the first studies to examine the decoding of more detailed movements non-invasively was conducted by Liao and colleagues (2014). Their subjects performed full finger extension and flexion movements repetitively when corresponding cues were presented. Movement-related power spectrums were identified through principal component analysis from high-density EEG data and binary classifications were done with a linear support vector machine. The first principal component showed highest decoding accuracy in all conditions compared to latter components with broadband spectrums always achieving higher accuracy than alpha,

beta or gamma band. However, similar results have been achieved in almost identical setups by using just alpha and beta band features (Lee et al. 2022; Xiao & Ding 2015).

A more comprehensive evaluation of EEG features in binary finger movement classification has shown that principal components of broadband power spectral densities indeed achieve highest decoding accuracies compared to all other features, at least when the first three components are used together. Moreover, accuracies of individual band powers seem to perform the worst. Surprisingly, temporal features yield slightly better results than individual principal components of broadband spectrums or band powers. (Xiao & Ding 2015)

Numerous features and classifiers have been employed to decode different forms of motion, as demonstrated through the preceding evidence. Both temporal and spectral characteristics have been extensively examined, consistently yielding accuracies that surpass the chance level. When decoding subtle finger movements, studies have predominantly relied on high-density signal acquisition and simple binary classifiers. Altogether, the viability of accurately categorizing a broad range of limb movements from brain signals has been effectively demonstrated.

5.2 Decoding continuous movements

Continuous decoding of limb movement is needed for a neuroprosthesis to work perfectly in an everyday environment. This means that velocity and position of the limb must be represented accurately in brain activity as a function of time. In these studies, three-dimensional velocity is usually enough to estimate continuous hand movement as position can be obtained by integrating velocity over time.

Bradberry and colleagues (2010) used a three-dimensional center-out paradigm in a reaching task to examine if hand velocity, measured by motion analysis, could be decoded from temporal features of sub 1 Hz EEG. A motion-sensing system tracked an LED placed on the subjects' fingertip as they reached to different targets. Correlations were computed between the measured hand velocities and the reconstructed velocities obtained via a linear regression model. The strongest correlations were observed in the sagittal (y) and vertical (z) directions (0.38 and 0.32, respectively), while the weakest correlation was found in the horizontal (x)

direction (0.19). Additionally, the researchers examined the impact of movement variability on decoding accuracy, revealing an expected reduction in accuracy with increased variation in the reaching trajectory.

Yeom et al. (2013) conducted a similar study but with MEG. They used stereographic images with 3D glasses to present spheres for the subjects to reach. Channels at the parietal lobe showed strong event-related synchronisation (ERS) at 0.5–8 Hz and moderate ERS at 57–98 Hz after movement onset. At the same time event-related desynchronisation (ERD) was prominent at 9–22 Hz. A multiple linear regression model was used to predict actual movement velocities from these frequency characteristics. Out of all frequency bands, only the theta band demonstrated consistent decoding capability. The correlations between the reconstructed velocities from the theta band and the measured velocities in the x, y, and z directions were 0.67, 0.70, and 0.75, respectively.

Frequency characteristics have also been used as a decoding feature with EEG. Korik et al. (2018) showed that when 3D reaching movements were decoded using linear regression, time-resolved power spectral density of the mu and beta bands showed higher decoding accuracy ($r = 0.40$) than standard low-pass filtered event-related potentials in the time domain ($r = 0.15$). In addition, with imagined movements all three bands showed higher accuracy ($r = 0.20$) than the time domain ($r \approx 0.01$).

In comparison to conventional linear regression models, non-linear approaches such as kernel ridge regression do not exhibit a notable superiority. However, the advantage of a non-linear model lies in its ability to achieve comparable performance using a smaller training dataset. Additionally, it has been observed that the linear model is more susceptible to the influence of eye movement artifacts, as their removal results in increased accuracy, while the same is not true for the non-linear model. (Wang et al. 2022)

One atypical feature that has been used for movement decoding is connectivity, which pertains to the synchronization of distinct brain regions. In a recent study by Hosseini et al. (2022), phase locking value (PLV) and magnitude squared coherence (MSC) were employed as measures of phase synchronization and frequency domain similarity. The setup involved four targets positioned within a horizontal 2D framework, with participants executing alternating reaches towards these targets. The researchers systematically explored all possible

combinations of EEG channel pairs to identify optimal pairs for both PLV and MSC, which were subsequently employed as features for multiple linear regression. The obtained average correlations of 0.43 and 0.42 were deemed superior to previously reported results achieved using alternative features, as highlighted by the authors.

5.3 Decoding sensory information

One of the few studies to examine the decoding of sensory stimuli applied to the fingers was done by Schroeder et al. (2017). They implanted rhesus macaques with microelectrode arrays and had them sit still in a chair when the macaques' fingers where individually either gently brushed or flexed and extended. In addition, the researchers trained them to do voluntarily finger movements to compare decoding accuracies between these conditions. Interestingly, they chose to use a Naïve Bayes algorithm to classify the fingers being stimulated with multiunit and single-unit recordings used as features.

The results demonstrated the presence of widespread tactile sensory responses in the hand area of the primary motor cortex, although the fraction of modulated units varied across macaques. The lack of somatotopic organization in the responses indicated that there is overlapping in the cortical representations of fingers. Furthermore, they found overlap in the sensory and motor responses which suggests that native sensory signals may contaminate motor signals and further emphasizes the integration of information in the cortex. Despite of this, the study successfully classified the stimulated finger based on firing rates, achieving above chance level decoding accuracies with both sensory modalities. (Schroeder et al. 2017)

Further investigations are warranted to determine optimal strategies for decoding subtle proprioceptive and tactile stimuli. To enable non-invasive neuroprosthetic BCIs to achieve superior levels of dexterity and precision, a thorough exploration of various features and decoding algorithms is essential to identify the most effective and practical solutions.

6 RESEARCH QUESTIONS AND HYPOTHESES

Question 1: Can proprioceptive or tactile stimuli applied to two different fingers be accurately decoded from MEG signals?

Hypothesis

Given the previous evidence regarding sensorimotor decoding (Liao et al. 2014; Xiao & Ding 2015), it is justifiable to assume that subtle stimuli of this nature can be accurately decoded from MEG. Research has demonstrated successful decoding of voluntary finger movements using non-invasive methods and tactile stimuli with invasive methods. Despite the detailed representation of fingers in the sensorimotor cortices, the spatial accuracy of MEG should be enough to detect these stimuli effectively.

Question 2: Can proprioceptive and tactile stimuli of the same finger be accurately decoded from MEG signals?

Hypothesis

According to the theory provided in chapter 3 (Graziano & Gross 1998; Johansson & Vallbo 1983; Kaas et al. 1993; Proske & Gandevia 2012), it can be reasonably assumed that the difference in cortical processing of proprioceptive and tactile stimuli is enough to cause sufficiently distinct MEG responses for this differentiation. From the literature review it is evident though, that there is a lack of studies that have tried to answer this particular question.

7 METHODS

7.1 Subjects, devices and measurement protocol

This study recruited ten healthy adults, each of whom provided informed consent in accordance with Declaration of Helsinki. The study was approved by the Ethics Committee of Aalto University. The experimental apparatus consisted of a specially constructed device designed to deliver sensory stimuli to the fingers of the participant's dominant hand (Figure 8). This device integrated a four-finger pneumatic movement actuator with a tactile stimulator (a small inflatable plastic film at the fingertip), configured to be compatible with the MEG system. Developed at Aalto NeuroImaging, Espoo, Finland, the device facilitated precise delivery of proprioceptive and tactile stimuli to the index, middle, ring, and little fingers.

Experiments were conducted at the MEG facility of Aalto NeuroImaging. The experimental setup targeted the aforementioned fingers, administering proprioceptive and tactile stimuli in a randomized sequence with a 2-second interstimulus interval. The design included eight stimulation categories, corresponding to each finger and two different conditions. A total of 400 trials were conducted—50 trials per category—to ensure the collection of sufficient data for robust analysis. Data recording was performed using a 306-channel Elekta Neuromag system (Elekta, Stockholm, Sweden), operating at a sampling rate of 1000 Hz.

FIGURE 8. Four-finger pneumatic actuator and tactile stimulator.

7.2 Preprocessing and selection of features

All of the preprocessing steps were done using specialized Python code and computer resources from Aalto University. In the initial phase of preprocessing, advanced noise reduction techniques were employed to enhance the signal quality. The first step involved using oversampled temporal projection (OTP), a method predicated on the assumption that the spatial distribution of sensors over-samples the signal space. Through this technique, each sensor's signal was reconstructed using the collective signals from other sensors, effectively filtering out temporally uncorrelated noise and improving the clarity of neuronal signals. (Larson & Taulu 2017)

Following OTP, temporal signal space separation (tSSS) was implemented to further mitigate external magnetic interferences and to compensate for any head movements during the recording. This step is critical as it ensures that the environmental noise and artifacts related to the subject's movement do not compromise the data integrity. (Taulu & Simola 2006) Additionally, the tSSS technique played a vital role in reconstructing signals from malfunctioning sensors, with typically 2 to 5 sensors requiring such intervention in each session to ensure comprehensive data coverage and consistency.

To address physiological artifacts such as eye blinks and cardiac signals, independent component analysis (ICA) was utilized. This method separates mixed signals into components based on their statistical independence (Barbati et al. 2004). The ocular components were identified with the aid of reference electrooculography (EOG) electrodes, ensuring precise delineation of eye-related artifacts. Moreover, all components identified for removal underwent manual verification to confirm their relevance to artifact rather than brain activity, underscoring the approach in preserving the integrity of neuronal signals in the processed MEG data.

A total of 92 gradiometer channels, 46 per side, were selected based on visual inspection of the event-related responses. Preference was given to channels located over the sensorimotor cortex that exhibited the highest amplitude peaks after stimulus onset. These temporal changes were then utilized as features for decoding. A sliding time window analysis was implemented, with the window set at 50 milliseconds and advancing in increments of 10 milliseconds from the stimulus onset up to 500 milliseconds post-stimulus.

7.3 Decoding algorithm and statistical analyses

A default support vector machine (SVM) was employed for decoding due to its efficacy and straightforward application in binary classification tasks. Initially, an equivalent number of trials were extracted from each of two datasets, representing different stimulus conditions. Subsequently, the data matrices were reshaped into vectors and subjected to random permutation. For validation, the data was partitioned into five equal subsets to facilitate 5-fold cross-validation. In this method, each subset was sequentially used as a testing set, while the remaining subsets were combined to form the training set. The SVM model was trained on these training sets, which included data from both conditions, and standardization was performed as part of the fitting process. Each fold involved running the classifier, using one fold for testing and the others for training. The performance of the model was evaluated by comparing the predicted labels against the actual labels of the testing set, with prediction accuracy calculated as a percentage for each fold. The mean prediction accuracy was then derived by averaging the accuracies obtained from all five folds.

The evaluation of the SVM model's performance was done through permutation testing. This involved merging the datasets and executing the permutation test 200 times, where the data was reshuffled and partitioned in each iteration. For each permutation, trials were randomly reassigned between the two datasets to simulate the null hypothesis that any differences observed between the groups were attributable to chance. Subsequently, each dataset permutation underwent the 5-fold cross-validation procedure. During each permutation and for each fold, data was split according to fold indices into training and testing sets. An SVM classifier was then trained using the training data and utilized to predict the labels of the testing data. The prediction accuracy for each fold was determined by comparing the predicted labels with the actual labels. This process resulted in a distribution of mean accuracies under the null hypothesis. From this distribution, the 95th percentile was computed, serving as the critical value for the significance test. An observed accuracy exceeding this critical value in a non-permuted experimental setup would indicate statistical significance at the 5% level. All computations were done using MATLAB R2023 (Mathworks Inc., US). Pseudo code is presented in Appendix A.

8 RESULTS

The selected MEG gradiometer channels and their spatial distribution on the scalp are highlighted in Figure 9. The same set of channels was used for all of the subjects. Both gradiometers from each sensor were included.

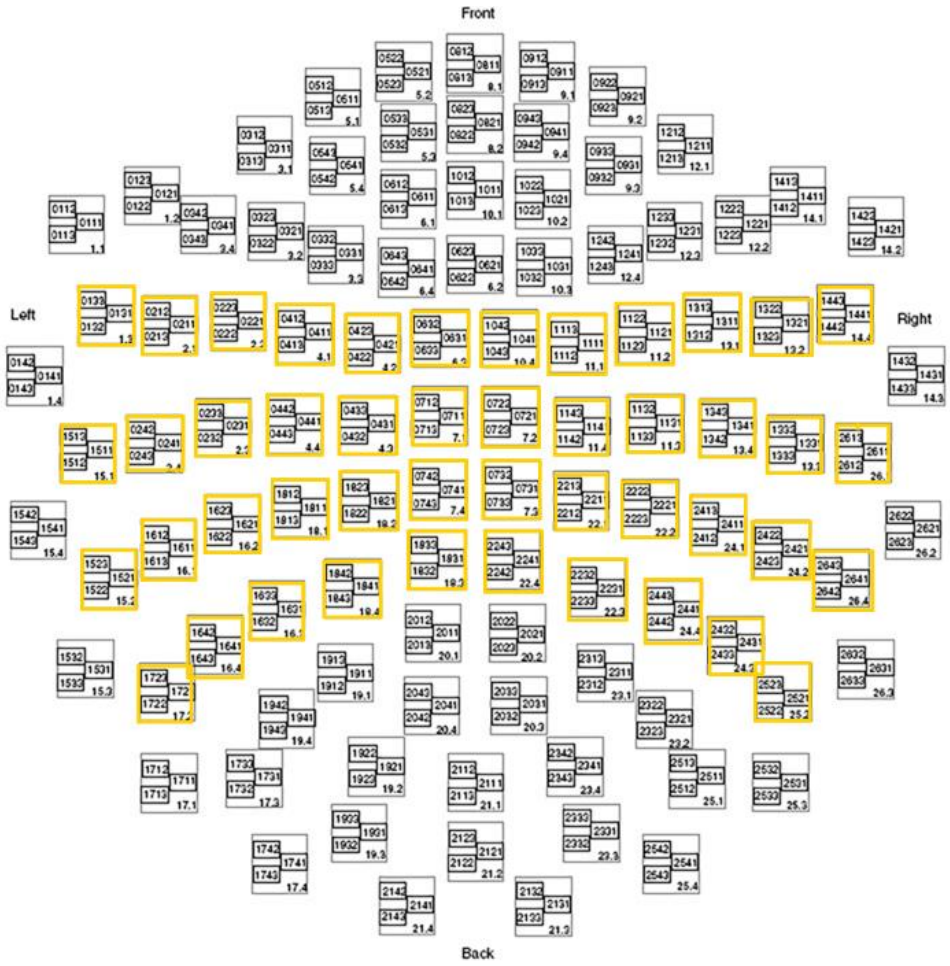

FIGURE 9. MEG channels selected for analysis.

The grand average responses to proprioceptive stimuli from all subjects, recorded at the selected channel (1812), are illustrated in Figure 10. The stimulus onset occurred at 0 ms. Consistent negative peaks appeared around 100 ms post-stimulus onset for the index, middle, and ring fingers. While the ring finger also exhibited this response, it was less pronounced. Additionally, the signal plateau towards the end of the time window was less evident. The peak amplitudes varied slightly, with the index finger showing the largest negative peak.

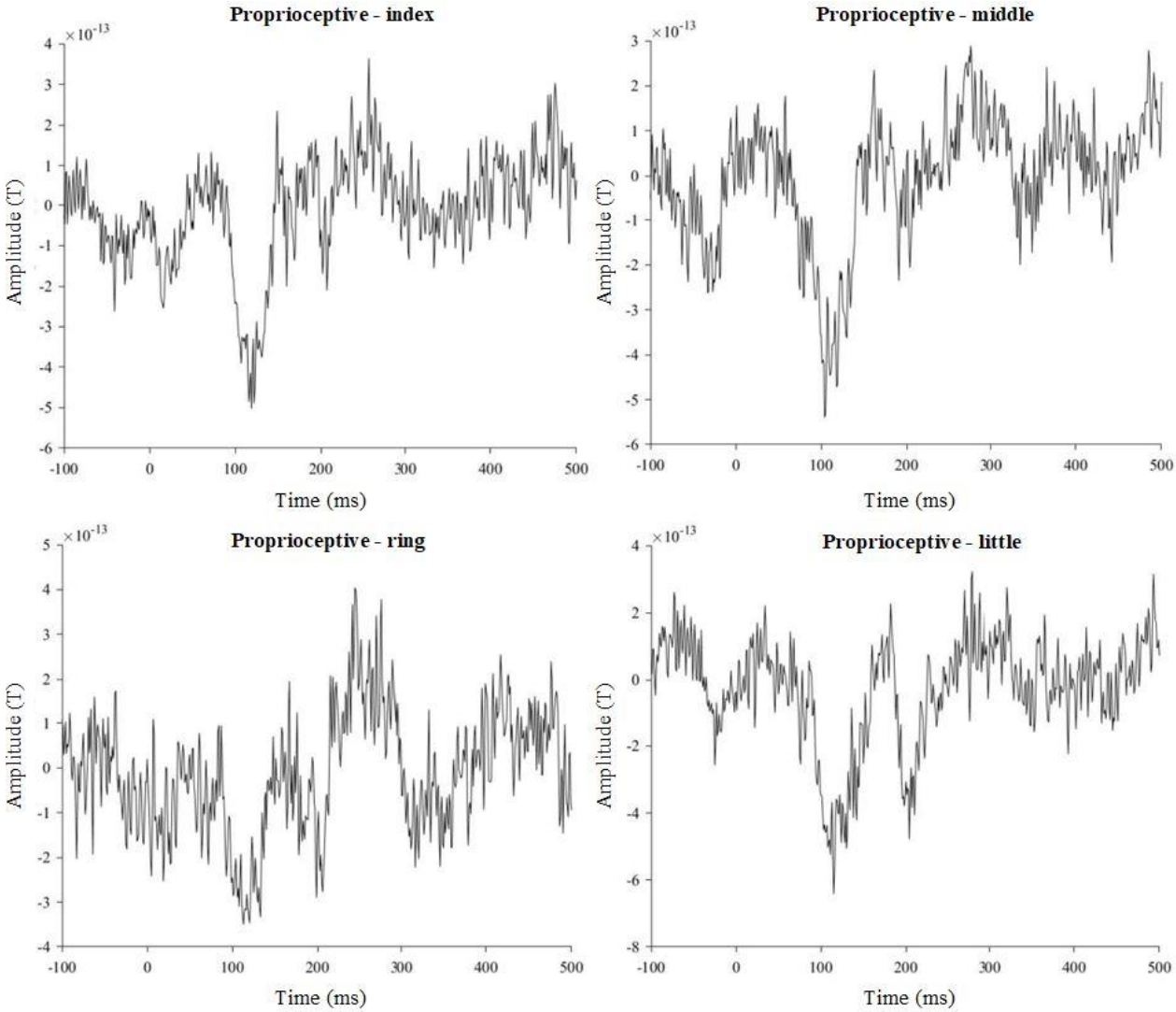

FIGURE 10. Grand average temporal responses for proprioceptive stimuli from a selected channel (1812).

The grand average responses to tactile stimuli from all subjects, recorded at the same channel, are shown in Figure 11. Similar negative peaks occurred at the same time point as with proprioceptive stimuli. However, the middle finger responses exhibited a more prominent negative-to-positive shift compared to the ring and little fingers. Unlike the proprioceptive stimuli, the tactile responses do not plateau as quickly towards the 500 ms mark at the end of the time window.

The 100 ms preceding the stimulus onset were relatively similar across all eight conditions. Nonetheless, some conditions displayed a subtle negative trend from the baseline.

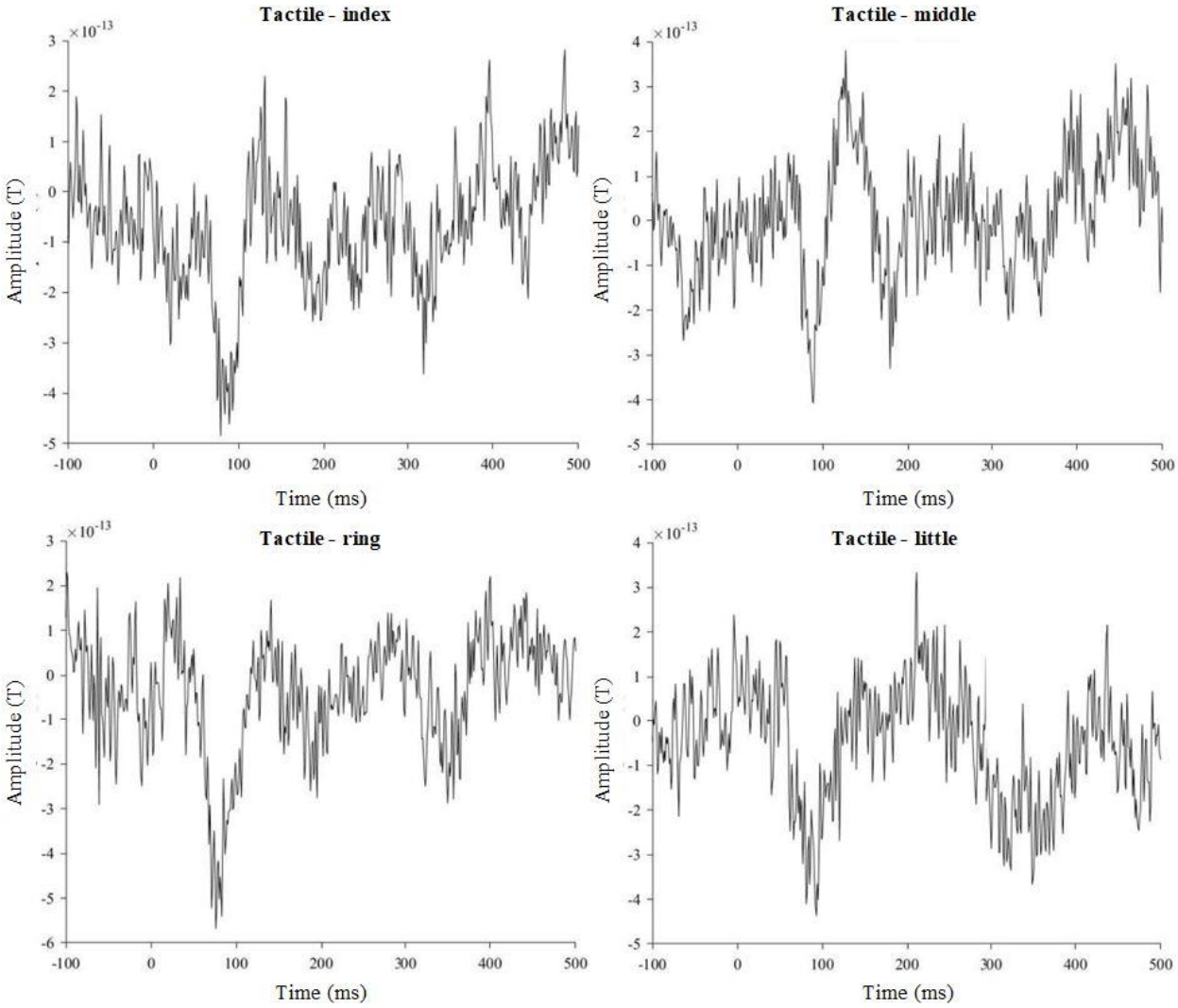

FIGURE 11. Grand average temporal responses for tactile stimuli from a selected channel (1812).

The results of the classifications between different fingers for each time window are presented in Figure 12. Three pairwise comparisons were conducted between the index finger and other fingers. All conditions exhibited similar trends, with increasing accuracies up to the 100 ms mark, achieving the highest accuracy just after this point in proprioceptive conditions. Interestingly, accuracies in tactile conditions increased more inconsistently, with peak accuracies detected just before the 100 ms mark. Classification in proprioceptive conditions was more consistent compared to tactile conditions. However, in both conditions, there was a scattering of accuracies towards the end of the time window.

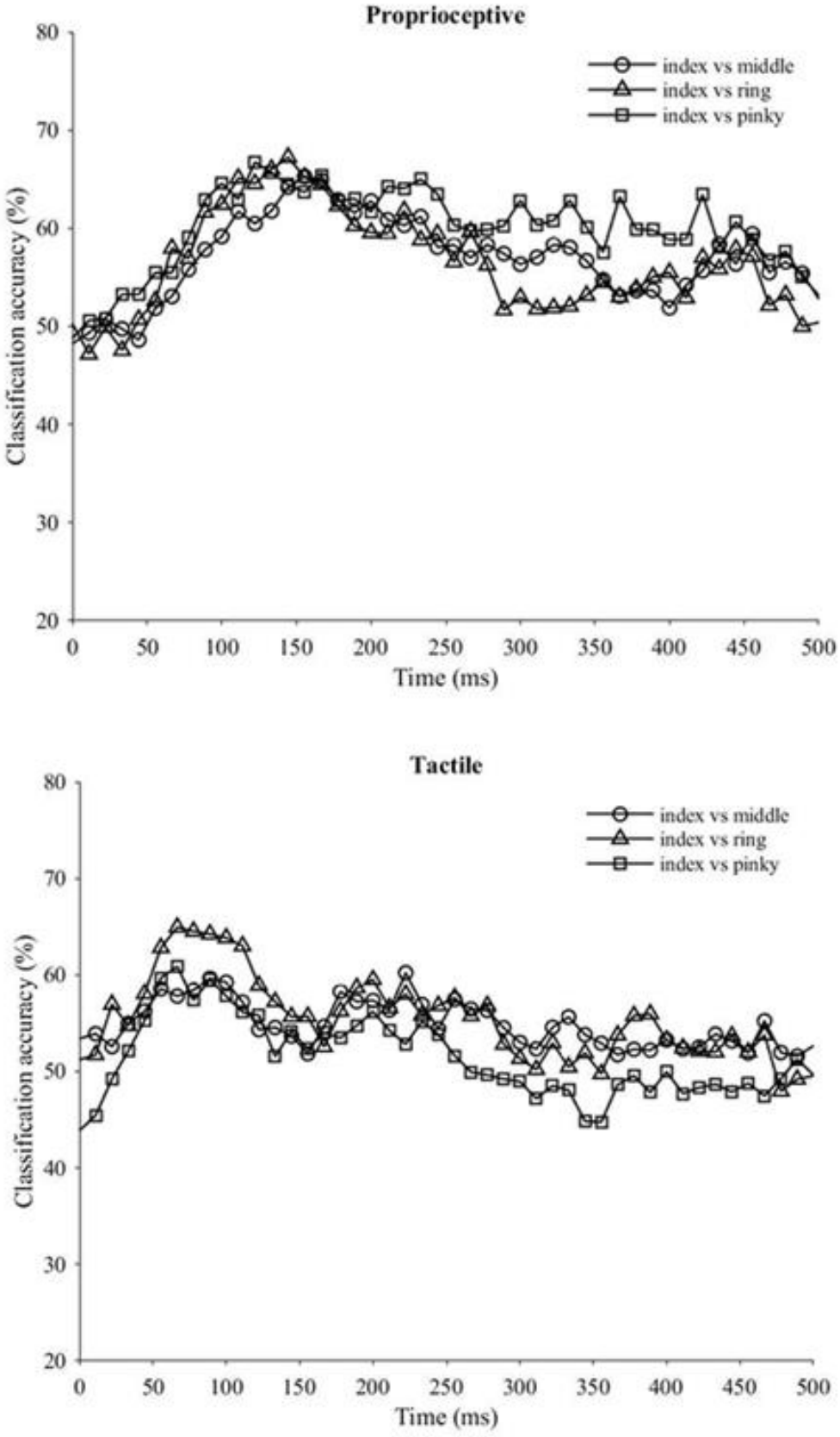

FIGURE 12. Grand average classification accuracies as a function of time for conditions between different fingers.

Interestingly, the classification accuracies of proprioceptive versus tactile stimuli (Figure 13) showed a very consistent increase towards the peak at the 100 ms mark, followed by a consistent decline. Notably, the highest accuracy achieved was slightly below 90%, which was significantly higher than the peak accuracies observed in other classification tasks.

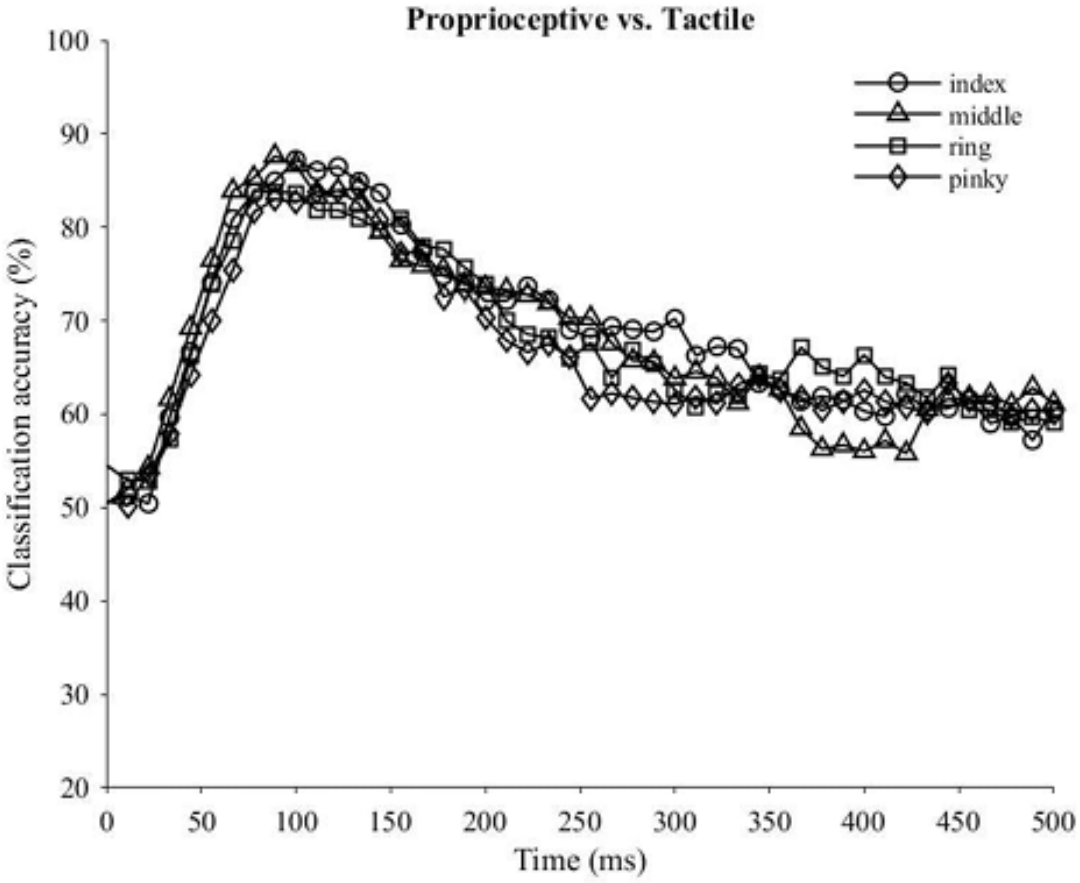

FIGURE 13. Grand average classification accuracies as a function of time for tactile versus proprioceptive stimulus conditions.

The highest classification accuracies were achieved at varying time points across different subjects. Tactile versus proprioceptive conditions exhibited significantly higher peak accuracies compared to other conditions, with some subjects reaching up to 99% accuracy. The mean of the highest accuracies was around 70% for conditions comparing different fingers and around 90% for tactile versus proprioceptive conditions. The latter also showed more consistent standard deviations of peak accuracies. Tables 1 and 2 present these peak accuracies and the corresponding 95% confidence intervals for all subjects.

TABLE 1. Highest decoding accuracies (%) and corresponding 95% confidence levels in conditions between different fingers.

	Proprioceptive			Tactile		
	index vs. middle	index vs. ring	index vs. pinky	index vs. middle	index vs. ring	index vs. pinky
Subject 1	74/59	73/58	75/59	64/59	67/58	72/58
Subject 2	66/58	67/59	69/57	68/59	74/57	76/56
Subject 3	68/59	61/57	61/59	69/58	64/58	69/58
Subject 4	74/59	71/58	74/59	70/58	77/59	77/60
Subject 5	73/58	72/57	77/57	65/60	63/58	68/59
Subject 6	80/58	84/59	89/60	77/57	83/59	79/59
Subject 7	70/58	66/59	67/59	65/58	71/58	72/59
Subject 8	72/58	88/59	75/59	65/58	82/59	71/59
Subject 9	65/59	73/59	80/58	72/59	72/59	71/58
Subject 10	62/58	70/59	68/59	64/59	66/58	71/58
Mean/SD	70.4/4.8	72.5/7.3	73.5/7.1	67.9/3.8	71.9/6.4	72.6/3.2

There were a few deviant observations; for example, subject 6 showed significantly higher peak accuracies compared to the rest. The lowest mean peak accuracy was observed in the index versus middle finger classification within the tactile category. However, all values exceeded the significance level across all conditions.

TABLE 2. Highest decoding accuracies (%) and corresponding 95% confidence levels in tactile versus proprioceptive stimulus conditions.

	Index	Middle	Ring	Pinky
Subject 1	92/60	86/58	90/58	92/60
Subject 2	90/58	90/57	85/58	84/57
Subject 3	83/60	81/58	82/59	73/59
Subject 4	90/58	87/59	84/58	86/58
Subject 5	79/58	79/59	75/60	81/60
Subject 6	99/58	99/59	94/58	90/60
Subject 7	94/59	95/59	92/57	85/58
Subject 8	95/58	96/59	99/58	95/60
Subject 9	94/57	96/57	96/58	91/59
Subject 10	99/58	94/59	93/60	94/58
Mean/SD	91.5/6.1	90.3/6.5	89.0/7.0	87.1/6.4

Subject 5 exhibited the lowest peak accuracies in tactile versus proprioceptive conditions, with values below 80%. The highest mean peak accuracy was observed for the index finger, while the middle, ring, and little fingers showed slightly declining results, respectively. Nevertheless, all values were above the significance level for these conditions as well.

Figure 14 illustrates the changes in decoding accuracy and its confidence level over time for subject 1 under various conditions. This figure highlights the differences in decoding performance between different stimuli and different fingers subjected to the same stimulus. Notably, the tactile stimuli applied to the index and middle fingers yielded very poor results for this subject, with nearly all time windows failing to produce significant classification accuracies.

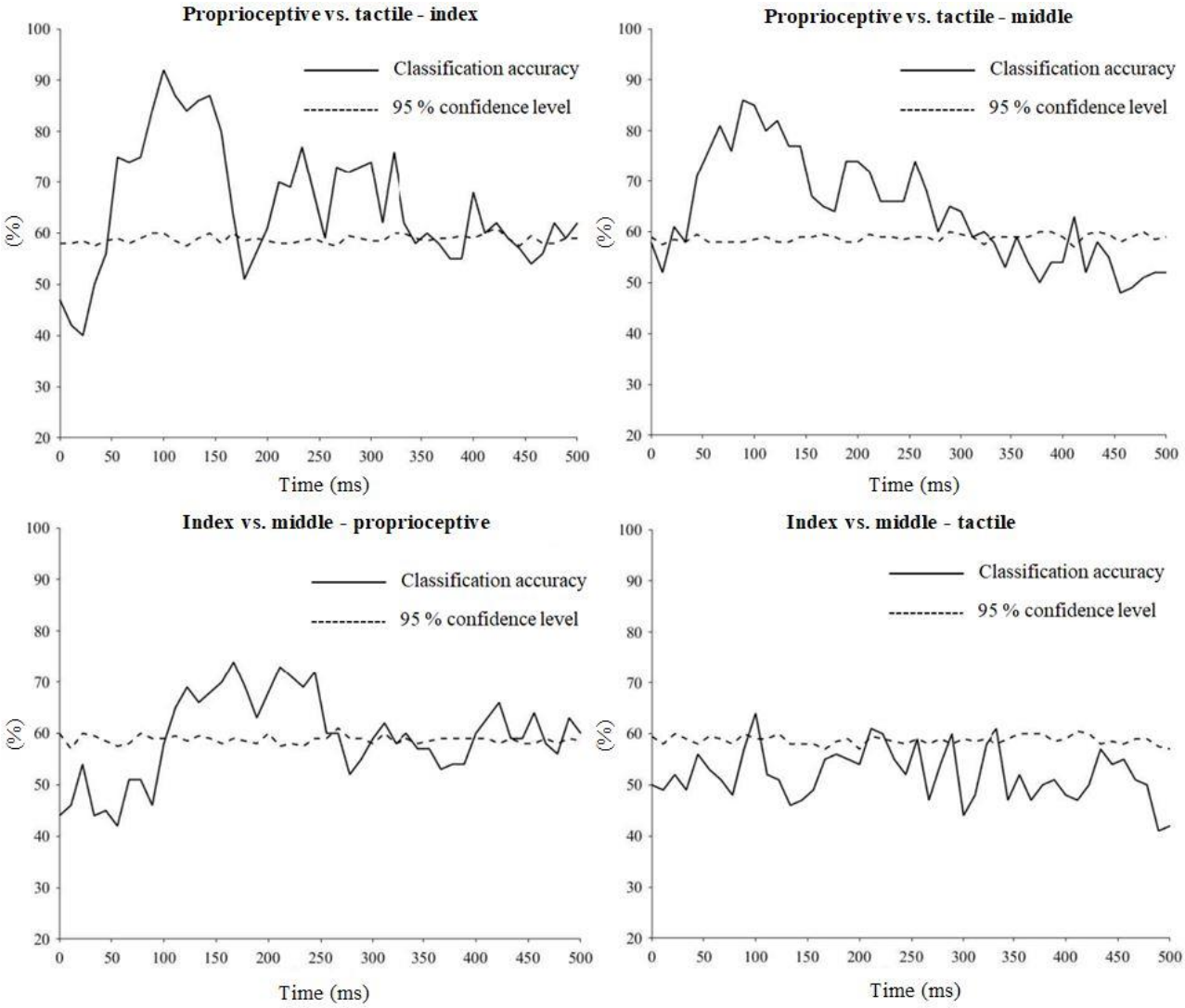

FIGURE 14. Selected classification accuracies and confidence levels from subject 1.

9 DISCUSSION

This study explored the feasibility of decoding proprioceptive and tactile stimuli applied to the fingers using a support vector machine for classification and MEG for signal acquisition. The temporal dynamics of MEG responses revealed consistent negative peaks around 100 milliseconds post-stimulus for both types of stimuli, with proprioceptive responses being more pronounced and consistent across fingers. The findings indicated that both proprioceptive and tactile stimuli could be accurately decoded when applied to different fingers, with proprioceptive stimuli generally yielding higher and more consistent accuracies. Classification accuracies for decoding proprioceptive stimuli applied to the index, middle, ring, and little fingers increased up to around 100 milliseconds post-stimulus, achieving peak accuracies shortly after this point, with mean peak accuracies ranging from approximately 66% to 84%. Tactile stimuli exhibited more variability in classification accuracies, peaking just before the 100 ms mark, with mean peak accuracies around 77%. Differentiating between proprioceptive and tactile stimuli applied to the same finger yielded higher accuracies, averaging around 90%, with some subjects achieving up to 99% accuracy.

9.1 Interpretation of the results

The neurophysiological differences between proprioceptive and tactile stimuli processing discussed in chapter 3 were not clearly reflected in the results. Contrary to expectations, the decoding accuracy peaked earlier for tactile conditions than for proprioceptive conditions. If the results had been reversed, this could have been attributed to the conduction velocities of Aβ and Ia afferents. As noted by Purves et al. (2018, 194), the conduction velocities for afferents conveying proprioceptive information range from 80 to 120 m/s, while for those conveying tactile information, they range from 30 to 70 m/s. This suggests that proprioceptive information would reach the brain more quickly after stimulus onset compared to tactile information, and thus, it would be expected that the decoding accuracy for proprioceptive stimuli would peak earlier than for tactile stimuli. However, given these conduction velocities, the difference in the time it takes for the signal to reach the brain is approximately 3 milliseconds. Consequently, the events occurring in the brain after the stimulus arrives may have a more substantial impact on the timing of the peak in decoding accuracy.

Interestingly, the grand average responses from the MEG signals did not show significant differences between tactile and proprioceptive conditions. Negative peaks at 100 ms post-stimulus onset were visible in all conditions, with only minor variations elsewhere. This could partly be attributed to the selection of channels, which were uniformly located over sensorimotor areas. If fewer channels had been selected, focusing only on the relevant areas, the average responses might have been more distinct between the conditions. Therefore, a valuable addition to this research would be to investigate the source space of the MEG data to provide more information about the spatial distribution of the responses and potentially improve decoding accuracy.

The most significant result was the decoding accuracies of proprioceptive and tactile stimuli applied to the same finger, which exceeded 90% for many subjects. This indicates that the underlying sensory processes for proprioceptive and tactile stimuli are fundamentally different. Although these differences were not visually evident in the averaged responses, the distinct sensory pathways and spatial separation of the processing layers in the brain (Graziano & Gross, 1998; Kaas et al., 1993) can be effectively captured by advanced machine learning methods like SVMs. Again, an interesting aspect would be to study the source space eventhough the sensory layers are in very close promixity.

The markedly lower accuracies in conditions involving different fingers could be attributed to the proximity of their respective processing areas in the brain, as highlighted in chapter 3 (Graziano & Gross 1998; Kaas et al. 1993). Additionally, the processing of proprioceptive stimuli for fingers like the index and middle finger might only differ in the location of their processing sites in the brain, rather than other factors such as temporal characteristics, as seen in different stimulus conditions. This is supported by the fact that higher peak decoding accuracies were observed for more distant finger pairs. Consequently, with MEG, the responses are not distinct enough to achieve high decoding accuracies, although some exceptions were observed in this dataset.

The anatomical structure of the muscle tendon units in the fingers can also influence these results. For instance, the flexor digitorum muscles flex all four fingers of the hand (Platzer 2015, 160-162), meaning that extending one finger will partially activate the same muscle spindles as extending other fingers. This overlap may contribute to the difficulty in classifying proprioceptive stimuli. However, this effect is not present with tactile stimuli.

Lastly, as illustrated in Figure 14, the decoding accuracies varied significantly across subjects and conditions, underscoring the individuality in responses to various stimuli. This variability highlights the complex nature of sensory processing and the influence of individual differences on decoding performance. Several factors could contribute to this individual variability, such as differences in the sensitivity of individuals to subtle sensory stimuli, variations in neural anatomy and physiology, and individual differences in cognitive and attentional states during the experiments.

9.2 Comparison with previous studies

Many previous brain signal decoding studies have utilized EEG due to its practicality in this context. Additionally, most of these studies have focused on the classification of gross upper limb movements, as discussed in chapter 4. Despite these differences, the results of this study are consistent with the findings from previous research.

Liao et al. (2014) studied the decoding of voluntary finger extension and flexion movements from EEG using principal components of the spectral density as feature for a linear SVM model. Their mean decoding accuracies for index finger versus middle, ring and little fingers were 69 %, 73 % and 79 %, respectively. Corresponding accuracies in the precent study were 70 %, 72 %, and 73 %. The only difference was the voluntary nature of movements in the study by Liao and collagues. This would seem to reflect the fact that proprioception is what carries most of the information for the decoding to reach high levels of accuracy since elicited movements alone can provide similar accuracies as voluntarily induced movements. This is further supported by the fact that imagined movements are less accurately decoded compared to executed movements (Kim et al. 2015, Korik et al. 2018).

Xiao and Ding (2013) employed similar methods to Liao et al. (2014) and demonstrated that dimension-reduced broadband spectral densities are the most effective features for decoding individual finger movements. In their study, some subjects achieved over 90% classification accuracy using the first principal components. This finding underscores the necessity of utilizing more robust features for accurately decoding finger movements, as relying solely on temporal response characteristics likely does not provide sufficient information for precise classification.

Overall, it appears that decoding finger movements under similar stimuli would benefit from different features compared to decoding different types of stimuli. The underlying differences in neural processing of proprioceptive and tactile stimuli seem to be sufficient to generate distinct temporal changes, making decoding feasible using only these temporal features. However, when decoding stimulated fingers from one another, it would be advantageous to use features that provide more comprehensive information, such as those obtained through PCA.

9.3 Methodological considerations

There were several methodological strengths and weaknesses in this study. One of the primary considerations is the delivery of the stimuli using the tactile stimulator. This device was designed to move the fingers taped to it and to deliver tactile stimuli by inflating a small plastic film. However, the device's construction may have caused the touch to elicit a subtle movement, potentially creating unintended proprioceptive stimuli, albeit much weaker than intentional movements. In theory, this could have influenced the decoding of different stimuli, but given that these conditions yielded the best results and the fact that the movement was almost negligible, it is likely that any unintended movements were not significantly problematic.

Another consideration is the potential for subjects to anticipate the incoming stimuli, thereby enhancing their neural responses. As indicated by previous studies, anticipatory activity or imagery alone can induce relevant changes in brain activity (Korik 2018; Piitulainen et al. 2021). However, this is mitigated by the fact the stimuli were completely randomized.

Variability in the results could have been reduced by including more subjects. With only ten participants, outliers can significantly impact overall results, and some of the deviations observed, particularly in tactile conditions, might have been mitigated with a larger sample size. Additionally, the number of trials per condition (50) could have been higher to improve classification robustness. Doubling the amount of trials and participants would probably improve the results without significant effort.

The preprocessing steps adhered to best practices, resulting in very clean raw data, which likely minimized any adverse effects on the results. However, the choice of channels for analysis could have influenced the outcomes. Although channels were visually selected based on the best responses, alternative channel selections might have improved accuracy.

A more robust analysis could have been achieved by using different time windows and step sizes. Due to resource limitations, a specific setup was chosen, but employing a growing window across a time region of interest could have provided more comprehensive data as features. Finally, exploring different feature selections might have further increased accuracy.

9.4 Practical applications

Based on the results of this study, the temporal characteristics of MEG signals used as features for SVMs can be highly effective in decoding proprioceptive and tactile stimuli applied to a single finger. Additionally, reasonable accuracy can be achieved in decoding sensory stimuli applied to different fingers. Therefore, future BCI applications could benefit from implementing decoders that utilize SVMs and temporal responses in brain signals.

To translate the findings of this study into practical applications, future research should investigate similar methods using EEG. EEG is also non-invasive and offers the additional practical advantage of being applicable in real-world BCI applications. Additionally, incorporating more complex feature selection procedures and potential multi-class classifiers could significantly improve results, thereby enhancing the versatility and effectiveness of future BCI applications.

10 CONCLUSIONS

This study demonstrated the feasibility of using MEG signals and SVMs to decode proprioceptive and tactile stimuli applied to the fingers. Temporal dynamics of MEG responses, particularly negative peaks around 100 milliseconds post-stimulus, effectively classified these stimuli, with proprioceptive stimuli yielding higher and more consistent accuracies (70%-73%) compared to tactile stimuli (67%-72%). Decoding accuracies for classifying stimuli applied to the same finger were even higher, averaging around 90%. Future research should expand the sample size, explore different feature selection methods, and consider using EEG for practical non-invasive BCI applications. Overall, the findings provide a solid foundation for advancing BCI technologies.

REFERENCES

Ajiboye, A. B., Willett, F. R., Young, D. R., Memberg, W. D., Murphy, B. A., Miller, J. P., … Kirsch, R. F. (2017). Restoration of reaching and grasping movements through brain-controlled muscle stimulation in a person with tetraplegia: A proof-of-concept demonstration. The Lancet, 389(10081), 1821–1830. doi: 10.1016/S0140-6736(17)30601-3

Alho, K., Winkler, I., Escera, C., Huotilainen, M., Virtanen, J., Jaaskelainen, I. P., … Ilmoniemi, R. J. (1998). Processing of novel sounds and frequency changes in the human auditory cortex: Magnetoencephalographic recordings. Psychophysiology, 35(2), 211–224. doi: 10.1111/1469-8986.3520211

Baillet, S. (2017). Magnetoencephalography for brain electrophysiology and imaging. Nature Neuroscience, 20(3), 327–339. doi: 10.1038/nn.4504

Barbati, G., Porcaro, C., Zappasodi, F., Rossini, P. & Tecchio, F. Optimization of an independent component analysis approach for artifact identification and removal in magnetoencephalographic signals. Clinical Neurophysiology, 115(5), 1220-32. doi: 10.1016/j.clinph.2003.12.015.

Bradberry, T. J., Gentili, R. J., & Contreras-Vidal, J. L. (2010). Reconstructing Three-Dimensional Hand Movements from Noninvasive Electroencephalographic Signals. The Journal of Neuroscience, 30(9), 3432–3437. doi: 10.1523/JNEUROSCI.6107-09.2010

Brenner, D., Lipton, J., Kaufman, L., & Williamson, S. J. (1978). Somatically Evoked Magnetic Fields of the Human Brain. Science, New Series, 199(4324), 81–83.

Buzsáki, G., & Draguhn, A. (2004). Neuronal Oscillations in Cortical Networks. Science, 304(5679), 1926–1929. doi: 10.1126/science.1099745

Chambers, M. R., Andres, K. H., Duering, M. V., & Iggo, A. (1972). The structure and

function of the slowly adapting type II mechanoreceptor in hairy skin. Quarterly Journal of Experimental Physiology and Cognate Medical Sciences, 57(4), 417–445. doi: 10.1113/expphysiol.1972.sp002177

Cohen, D. (1972). Magnetoencephalography: Detection of the Brain's Electrical Activity with a Superconducting Magnetometer. Science, New Series, 175(4022), 664–666.

Cohen, M. X. (2014). Analyzing neural time series data: Theory and practice. Cambridge, Massachusetts: The MIT Press.

Edin, B. B. (1992). Quantitative analysis of static strain sensitivity in human mechanoreceptors from hairy skin. Journal of Neurophysiology, 67(5), 1105–1113. doi: 10.1152/jn.1992.67.5.1105

Edin, Benoni B. (2004). Quantitative Analyses of Dynamic Strain Sensitivity in Human Skin Mechanoreceptors. Journal of Neurophysiology, 92(6), 3233–3243. doi: 10.1152/jn.00628.2004

Graziano, M. S., & Gross, C. G. (1998). Spatial maps for the control of movement. Current Opinion in Neurobiology, 8(2), 195–201. doi: 10.1016/S0959-4388(98)80140-2

Gross, J., Baillet, S., Barnes, G. R., Henson, R. N., Hillebrand, A., Jensen, O., … Schoffelen, J.-M. (2013). Good practice for conducting and reporting MEG research. NeuroImage, 65, 349–363. doi: 10.1016/j.neuroimage.2012.10.001

Gujarati, D. N. (2018). Linear Regression: A Mathematical Introduction. 1st edition. California: SAGE Publications.

Hari, R. (1984). Somatosensory evoked cerebral magnetic fields from SI and SII in man. Electroeneephalography and Clinical Neurophysiology, 57, 254-263.

Haumann, N. T., Parkkonen, L., Kliuchko, M., Vuust, P., & Brattico, E. (2016). Comparing the Performance of Popular MEG/EEG Artifact Correction Methods in an Evoked-Response Study. Computational Intelligence and Neuroscience, 2016, 1–10. doi: 10.1155/2016/7489108

Hodgkin, A. L. (1951). The ionic basis of electrical activity in nerve and muscle. Biological Reviews, 26(4), 339–409. doi: 10.1111/j.1469-185X.1951.tb01204.x

Hosseini, S. M., & Shalchyan, V. (2022). Continuous Decoding of Hand Movement From EEG Signals Using Phase-Based Connectivity Features. Frontiers in Human Neuroscience, 16, 901285. doi: 10.3389/fnhum.2022.901285

Hunt, C. C., & McIntyre, A. K. (1960). Properties of cutaneous touch receptors in cat. The Journal of Physiology, 153(1), 88–98. doi: 10.1113/jphysiol.1960.sp006520

Hämäläinen, M., Hari, R., Ilmoniemi, R. J., Knuutila, J., & Lounasmaa, O. V. (1993). Magnetoencephalography—Theory, instrumentation, and applications to noninvasive studies of the working human brain. Reviews of Modern Physics, 65(2), 413–497. doi: 10.1103/RevModPhys.65.413

Hämäläinen, M. S. (1992). Magnetoencephalography: A tool for functional brain imaging. Brain Topography, 5(2), 95–102. doi: 10.1007/BF01129036

Iggo, A., & Muir, A. R. (1969). The structure and function of a slowly adapting touch corpuscle in hairy skin. The Journal of Physiology, 200(3), 763–796. doi: 10.1113/jphysiol.1969.sp008721

Johansson, R. S., & Flanagan, J. R. (2009). Coding and use of tactile signals from the fingertips in object manipulation tasks. Nature Reviews Neuroscience, 10(5), 345–359. doi: 10.1038/nrn2621

Johansson, R. S., & Vallbo, Å. B. (1983). Tactile sensory coding in the glabrous skin of the human hand. Trends in Neurosciences.

Jung, A. (2022). Machine Learning: The Basics. Singapore: Springer Nature Singapore. doi: 10.1007/978-981-16-8193-6

Kaas, J. H. (1993). The functional organization of somatosensory cortex in primates. Annals of Anatomy - Anatomischer Anzeiger, 175(6), 509–518. doi: 10.1016/S0940-

9602(11)80212-8

Kantzanou, M., Korfias, S., Panourias, I., Sakas, D. E., & Karalexi, M. A. (2021). Deep Brain Stimulation-Related Surgical Site Infections: A Systematic Review and Meta-Analysis. Neuromodulation: Technology at the Neural Interface, 24(2), 197–211. doi: 10.1111/ner.13354

Kim, J.-H., Biessmann, F., & Lee, S.-W. (2015). Decoding Three-Dimensional Trajectory of Executed and Imagined Arm Movements From Electroencephalogram Signals. IEEE Transactions on Neural Systems and Rehabilitation Engineering, 23(5), 867–876. doi: 10.1109/TNSRE.2014.2375879

Klimesch, W. (1999). EEG alpha and theta oscillations reflect cognitive and memory performance: A review and analysis. Brain Research Reviews, 29(2–3), 169–195. doi: 10.1016/S0165-0173(98)00056-3

Korik, A., Sosnik, R., Siddique, N., & Coyle, D. (2018). Decoding Imagined 3D Hand Movement Trajectories From EEG: Evidence to Support the Use of Mu, Beta, and Low Gamma Oscillations. Frontiers in Neuroscience, 12, 130. doi: 10.3389/fnins.2018.00130

Larson, E. & Taulu, S. (2017). Reducing Sensor Noise in MEG and EEG Recordings Using Oversampled Temporal Projection. IEEE Transactions on Biomedical Engineering, 65(5), 1003-1013. doi: 10.1109/TBME.2017.2734641

Lee, H. S., Schreiner, L., Jo, S.-H., Sieghartsleitner, S., Jordan, M., Pretl, H., … Park, H.-S. (2022). Individual finger movement decoding using a novel ultra-high-density electroencephalography-based brain-computer interface system. Frontiers in Neuroscience, 16, 1009878. doi: 10.3389/fnins.2022.1009878

Lee, Y. & Kim, K. (2014). Instrumentation for Measuring MEG Signals. In S. Supek & C. J. Aine (edit.) Magnetoencephalography – From Signals to Dynamic Cortical Networks. 1st edition. London: Springer, 3-33.

Liao, K., Xiao, R., Gonzalez, J., & Ding, L. (2014). Decoding Individual Finger Movements from One Hand Using Human EEG Signals. PLoS ONE, 9(1), e85192. doi: 10.1371/journal.pone.0085192

Matthews, P. B. C. (1991). The human stretch reltex and the motor cortex. Trends in Neurosciences, 14(3), 87-91.

Miller, K. J., Leuthardt, E. C., Schalk, G., Rao, R. P. N., Anderson, N. R., Moran, D. W., … Ojemann, J. G. (2007). Spectral Changes in Cortical Surface Potentials during Motor Movement. The Journal of Neuroscience, 27(9), 2424–2432. doi: 10.1523/JNEUROSCI.3886-06.2007

Miller, K. J., Schalk, G., Fetz, E. E., Den Nijs, M., Ojemann, J. G., & Rao, R. P. N. (2010). Cortical activity during motor execution, motor imagery, and imagery-based online feedback. Proceedings of the National Academy of Sciences, 107(9), 4430–4435. doi: 10.1073/pnas.0913697107

Murtagh, F. (1991). Multilayer perceptrons for classification and regression. Neurocomputing, 2(5–6), 183–197. doi: 10.1016/0925-2312(91)90023-5

Nason, S. R., Mender, M. J., Letner, J. G., Chestek, C. A., & Patil, P. G. (2021). Restoring upper extremity function with brain-machine interfaces. Teoksessa International Review of Neurobiology (Vsk. 159, ss. 153–186). Elsevier. doi: 10.1016/bs.irn.2021.06.001

Nielsen, M. (2015). Neural Networks and Deep Learning. Determination Press. Cited 1.6.2023. http://neuralnetworksanddeeplearning.com/chap1.html

Näätänen, R., Paavilainen, P., Rinne, T., & Alho, K. (2007). The mismatch negativity (MMN)

in basic research of central auditory processing: A review. Clinical Neurophysiology, 118(12), 2544–2590. doi: 10.1016/j.clinph.2007.04.026

Okada, Y. C., Tanenbaum, R., Williamson, S. J., & Kaufman, L. (1984). Somatotopic organization of the human somatosensory cortex revealed by neuromagnetic measurements. Experimental Brain Research, 56(2). doi: 10.1007/BF00236274

Piitulainen, H., Nurmi, T. & Hakonen, M. (2021). Attention directed to proprioceptive stimulation alters its corticalprocessing in the primary sensorimotor cortex. European Journal of Neuroscience, 54, 4269–4282. doi: 10.1111/ejn.15251

Platzer, W. (2015). Color Atlas of Human Anatomy – Vol. 1 Locomotor System. Seventh Edition. Stuttgart, Germany: Thieme.

Proske, U., & Gandevia, S. C. (2012). The Proprioceptive Senses: Their Roles in Signaling Body Shape, Body Position and Movement, and Muscle Force. Physiological Reviews, 92(4), 1651–1697. doi: 10.1152/physrev.00048.2011

Purves, D., Augustine, G. J., Fitzpatrick, D., Hall, W. C., Lamantia, A., Mooney, R. D., Platt, M. L. & White, L. E. (2018). Neuroscience. Sixth Edition. Cary, NC: Oxford University Press.

Ryhönen, T., Seppä, H., Ilmoniemi, R., & Knuutila, J. (1989). SQUID magnetometers for low-frequency applications. Journal of Low Temperature Physics, 76(5–6), 287–386. doi: 10.1007/BF00681735

Schroeder, K. E., Irwin, Z. T., Bullard, A. J., Thompson, D. E., Bentley, J. N., Stacey, W. C., … Chestek, C. A. (2017). Robust tactile sensory responses in finger area of primate motor cortex relevant to prosthetic control. Journal of Neural Engineering, 14(4), 046016. doi: 10.1088/1741-2552/aa7329

Schwarz, A., Ofner, P., Pereira, J., Sburlea, A. I., & Müller-Putz, G. R. (2018). Decoding natural reach-and-grasp actions from human EEG. Journal of Neural Engineering,

15(1), 016005. doi: 10.1088/1741-2552/aa8911

Shefner, J. M., & Logician, E. L. (1994). Conduction velocity in motor, cutaneous afferent, and muscle afferent fibers within the same mixed nerve. Muscle & Nerve, 17(7), 773–778. doi: 10.1002/mus.880170712

Sutton, S., Braren, M., Zubin, J., & John, E. R. (1965). Evoked-Potential Correlates of Stimulus Uncertainty. Science, New Series, 150(3700), 1187–1188.

Syukens, J. A. K., Van Gestel, T., De Brabanter, J., De Moor, B. & Vandewalle, J. (2002). Least Squares Support Vector Machines. 1st edition. Singapore: World Scientific Publishing.

Taulu, S. & Simola, J. (2006). Spatiotemporal signal space separation method for rejecting nearby interference in MEG measurements. Physics in Medicine and Biology, 51(7), 1759-68. doi: 10.1088/0031-9155/51/7/008

Tharwat, A., Gaber, T., Ibrahim, A., & Hassanien, A. E. (2017). Linear discriminant analysis: A detailed tutorial. AI Communications, 30(2), 169–190. doi: 10.3233/AIC-170729

Waldert, S., Pistohl, T., Braun, C., Ball, T., Aertsen, A., & Mehring, C. (2009). A review on directional information in neural signals for brain-machine interfaces. Journal of Physiology-Paris, 103(3–5), 244–254. doi: 10.1016/j.jphysparis.2009.08.007

Waldert, S., Preissl, H., Demandt, E., Braun, C., Birbaumer, N., Aertsen, A., & Mehring, C. (2008). Hand Movement Direction Decoded from MEG and EEG. The Journal of Neuroscience, 28(4), 1000–1008. doi: 10.1523/JNEUROSCI.5171-07.2008

Wang, J., Bi, L., Fei, W., & Tian, K. (2022). EEG-Based Continuous Hand Movement Decoding Using Improved Center-Out Paradigm. IEEE Transactions on Neural Systems and Rehabilitation Engineering, 30, 2845–2855. doi: 10.1109/TNSRE.2022.3211276

Xiao, R., & Ding, L. (2015). EEG resolutions in detecting and decoding finger movements

from spectral analysis. Frontiers in Neuroscience, 9. doi: 10.3389/fnins.2015.00308

Xu, B., Wang, Y., Deng, L., Wu, C., Zhang, W., Li, H., & Song, A. (2021a). Decoding Hand Movement Types and Kinematic Information From Electroencephalogram. IEEE Transactions on Neural Systems and Rehabilitation Engineering, 29, 1744–1755. doi: 10.1109/TNSRE.2021.3106897

Xu, B., Zhang, D., Wang, Y., Deng, L., Wang, X., Wu, C., & Song, A. (2021b). Decoding Different Reach-and-Grasp Movements Using Noninvasive Electroencephalogram. Frontiers in Neuroscience, 15, 684547. doi: 10.3389/fnins.2021.684547

Yeom, H. G., Kim, J. S., & Chung, C. K. (2013). Estimation of the velocity and trajectory of three-dimensional reaching movements from non-invasive magnetoencephalography signals. Journal of Neural Engineering, 10(2), 026006. doi: 10.1088/1741-2560/10/2/026006

Zimmerman, J. E., Thiene, P., & Harding, J. T. (1970). Design and Operation of Stable rf-Biased Superconducting Point-Contact Quantum Devices, and a Note on the Properties of Perfectly Clean Metal Contacts. Journal of Applied Physics, 41(4), 1572–1580. doi: 10.1063/1.1659074

APPENDIX A. Pseudo code for SVM model and its validation.

```
% Add necessary paths for functions
addPath('mneM');

% Define input file path
inputFile = 'path/to/your/file.fif';

% Set up reading the raw data from fif file
raw = setupReadRaw(inputFile);

% Define the channels of interest for tactile and actuator stimuli
includeSTI = {'STI101', 'STI005', 'STI006', 'STI007', 'STI008', 'STI009', 'STI010', 'STI011',
'STI012'};

% Pick specific channels for index and little finger tactile stimuli
picksSTI1 = pickTypes(raw.info, 0, 0, 0, includeSTI[2]);
picksSTI2 = pickTypes(raw.info, 0, 0, 0, includeSTI[5]);

% Read raw data segments for the selected channels
data1 = readRawSegmentDebug(raw, picksSTI1);
data2 = readRawSegmentDebug(raw, picksSTI2);

% Ensure the data matrices are the same size
minSize = min(size(data1,1), size(data2,1));
data1_d = data1(1:minSize,:,:);
data2_d = data2(1:minSize,:,:);

% Reshape matrices into vectors
data1_d = reshape(data1_d, size(data1_d,1), size(data1_d,2)*size(data1_d,3));
data2_d = reshape(data2_d, size(data2_d,1), size(data2_d,2)*size(data2_d,3));

% Randomly permute the data
permIndices = randperm(minSize);
```

```
data1_d = data1_d(permIndices,:);
data2_d = data2_d(permIndices,:);

% Define the number of folds for cross-validation
foldNum = 5;
foldSize = floor(minSize / foldNum);
foldIndices = zeros(foldNum, foldSize);

% Assign indices for each fold
for n = 1 to foldNum do
  foldIndices(n,:) = ((n-1) * foldSize + 1) to (n * foldSize);
end for

% Adjust data matrices to include only the trials that fit into the folds
x1 = foldNum * foldSize;
data1_d = data1_d(1:x1,:);
data2_d = data2_d(1:x1,:);

% Perform classification using 5-fold cross-validation
for k = 1 to foldNum do
 % Determine training and testing indices
 trainIndices = [];
 for n = 1 to foldNum do
   if (k != n) then
     trainIndices.append(foldIndices(n,:));
   end if
 end for
 testIndices = foldIndices(k,:);

 % Separate training and testing data
 data1a = data1_d(trainIndices,:);
 data2a = data2_d(trainIndices,:);
 data1b = data1_d(testIndices,:);
 data2b = data2_d(testIndices,:);
```

```
  % Train SVM model
  X = concatenate(data1a, data2a);
  Y = concatenate(ones(size(data1a,1),1), 2*ones(size(data2a,1),1));
  SVMModel = fitSVM(X, Y, 'Standardize', true);

  % Test the model and predict labels
  newX = concatenate(data1b, data2b);
  newY = concatenate(ones(size(data1b,1),1), 2*ones(size(data2b,1),1));
  [label, score] = predict(SVMModel, newX);

  % Store prediction accuracy for this fold
  pred(k) = 100 * (sum(label == newY) / (2 * foldSize));
end for

% Calculate mean classification accuracy across folds
predMean = mean(pred);

% Perform significance testing with permutation
dataAll = concatenate(data1_d, data2_d);
for l = 1 to 200 do
    permIndices = randperm(x1*2);
    data1_p = dataAll(permIndices(1:x1),:);
    data2_p = dataAll(permIndices(x1+1:end),:);
    for k = 1 to foldNum do
      trainIndices = [];
      for n = 1 to foldNum do
        if (k != n) then
          trainIndices.append(foldIndices(n,:));
        end if
      end for
      testIndices = foldIndices(k,:);

      data1a = data1_p(trainIndices,:);
      data2a = data2_p(trainIndices,:);
```

```
        data1b = data1_p(testIndices,:);
        data2b = data2_p(testIndices,:);

        X = concatenate(data1a, data2a);
        Y = concatenate(ones(size(data1a,1),1), 2*ones(size(data2a,1),1));

        SVMModel = fitSVM(X, Y, 'Standardize', true);
        newX = concatenate(data1b, data2b);
        newY = concatenate(ones(size(data1b,1),1), 2*ones(size(data2b,1),1));
        [label, score] = predict(SVMModel, newX);
        pred(k) = 100 * (sum(label == newY) / (2 * foldSize));
    end for
    predPercentile(l) = mean(pred);
end for

% Calculate the 95th percentile confidence interval
conf95 = percentile(predPercentile, 95);
```